

# The maternal vaginal microbiome partially mediates the effects of prenatal stress on offspring gut and hypothalamus

Eldin Jašarević<sup>1,2,3,4</sup>, Christopher D. Howard<sup>1,2</sup>, Kathleen Morrison<sup>1,2,3,4</sup>, Ana Misić<sup>1,5</sup>, Tiffany Weinkopff<sup>3</sup>, Phillip Scott<sup>1,3</sup>, Christopher Hunter<sup>1,3</sup>, Daniel Beiting<sup>1,3</sup> and Tracy L. Bale<sup>1,2,3,4\*</sup>

**Early prenatal stress disrupts maternal-to-offspring microbiota transmission and has lasting effects on metabolism, physiology, cognition, and behavior in male mice. Here we show that transplantation of maternal vaginal microbiota from stressed dams into naive pups delivered by cesarean section had effects that partly resembled those seen in prenatally stressed males. However, transplantation of control maternal vaginal microbiota into prenatally stressed pups delivered by cesarean section did not rescue the prenatal-stress phenotype. Prenatal stress was associated with alterations in the fetal intestinal transcriptome and niche, as well as with changes in the adult gut that were altered by additional stress exposure in adulthood. Further, maternal vaginal transfer also partially mediated the effects of prenatal stress on hypothalamic gene expression, as observed after chronic stress in adulthood. These findings suggest that the maternal vaginal microbiota contribute to the lasting effects of prenatal stress on gut and hypothalamus in male mice.**

Maternal stress experience during pregnancy is a risk factor for neurodevelopmental and gastrointestinal disorders in the offspring, yet the exact underlying mechanisms remain elusive<sup>1</sup>. Recent reports have demonstrated an association between the developing brain and the initial bacterial communities established within the gastrointestinal tract, whereby brain areas that control stress-related behaviors are modulated by signals derived from the gut microbiome<sup>2–6</sup>. The pioneer community of maternal microbiota that colonizes the offspring gastrointestinal tract at birth has a lasting impact on the gut and brain<sup>7–9</sup>. Therefore, if maternal perturbations, such as stress, alter the vaginal microbial composition during pregnancy, these communities may be transferred to her offspring at birth. Colonization by stress-altered communities may affect the postnatal development of systems that determine how the offspring will respond to the environment throughout life, including the brain, gut, immune system, and metabolic system<sup>7–9</sup>.

Using our well-established mouse model of early prenatal stress, we previously demonstrated that maternal stress exposure during pregnancy produced lasting changes to the maternal vaginal microbiome and consequently altered the composition of microbiota colonizing the neonatal gut<sup>10,11</sup>. Consistent with the role of gut microbiota in immune and metabolic functioning, we reported that prenatal-stress-induced changes in the colonizing microbiota were associated with altered metabolite profiles in the neonate's gut and hypothalamus<sup>11</sup>. In addition, in adulthood, prenatal-stress-exposed males (but not females) had reduced body weight, an increased neuroendocrine response to acute stressors, increased anhedonia, and altered stress-related gene expression in the hypothalamus<sup>12–16</sup>. These previous studies found no effects of prenatal stress in female offspring<sup>12–16</sup>.

As maternal stress exposure has disruptive effects on both the in utero environment and maternal microbial communities<sup>10–12</sup>, it has been difficult to assess the mechanistic involvement of the maternal vaginal microbiome to the prenatal stress phenotype independent of stress effects on the prenatal environment. To determine whether the maternal vaginal microbiome mediates the effects of prenatal stress on the offspring, we used cesarean delivery and neonate oral gavage from control and prenatal-stress-exposed dams to manipulate the colonizing microbiota. To control for the effects of the postnatal environment and housing conditions in these studies, offspring were tattooed and cross-fostered to a surrogate dam, with both sexes and all treatment groups represented in the litter. In adulthood, offspring were assessed for a rescue or recapitulation of the prenatal stress phenotype (Fig. 1a).

## Results

**Maternal vaginal microbiota modulate effects of prenatal stress on neonatal gut microbiota composition.** Clinical reports have shown that cesarean surgery prevents the natural colonization of the infant gut by the maternal vaginal microbiota, which can be restored by exposing the neonate to maternal vaginal fluids at birth<sup>17,18</sup>. These data suggest that cesarean surgery procedures could be leveraged as an experimental method to manipulate the colonizing microbiota composition to assess whether the transmission of maternal microbiota exerts lasting effects on offspring. We developed a vaginal microbiota transplantation approach, in which embryonic day (E) 18.5 mouse pups were delivered by cesarean section and exposed to a maternal vaginal inoculant via orogastric gavage (Fig. 1a). As cross-fostering and co-housing are themselves sufficient to transfer phenotypes<sup>19</sup>, we controlled for the effects of the postnatal environment and housing conditions by cross-fostering both sexes

<sup>1</sup>Center for Host-Microbial Interactions, University of Pennsylvania, Philadelphia, PA, USA. <sup>2</sup>Department of Biomedical Sciences, University of Pennsylvania, Philadelphia, PA, USA. <sup>3</sup>Department of Pharmacology, University of Maryland, Baltimore, MD, USA. <sup>4</sup>Center for Epigenetic Research in Child Health and Brain Development, School of Medicine, University of Maryland, Baltimore, MD, USA. <sup>5</sup>Department of Pathobiology, School of Veterinary Medicine, University of Pennsylvania, Philadelphia, PA, USA. \*e-mail: [TBale@som.umaryland.edu](mailto:TBale@som.umaryland.edu)

and all treatment groups to surrogate dams<sup>19</sup>. To confirm that the offspring gut microbiota are directly influenced by vertical transmission of maternal vaginal microbiota, we compared postnatal day (P) 2 gut microbiota between vaginally delivered offspring with offspring delivered by cesarean that were not inoculated with maternal vaginal fluid. Noninoculated cesarean-delivered offspring showed significant shifts in the composition of gut microbiota relative to vaginally delivered offspring (Fig. 1b,c). Microbiota diversity was also significantly decreased in noninoculated cesarean delivered offspring compared with vaginally delivered offspring at P2 (Fig. 1c,d). Notably, microbial diversity, structure, and composition at P2 were similar in inoculated cesarean-delivered offspring and vaginally delivered offspring (Fig. 1c,d and Supplementary Fig. 1a).

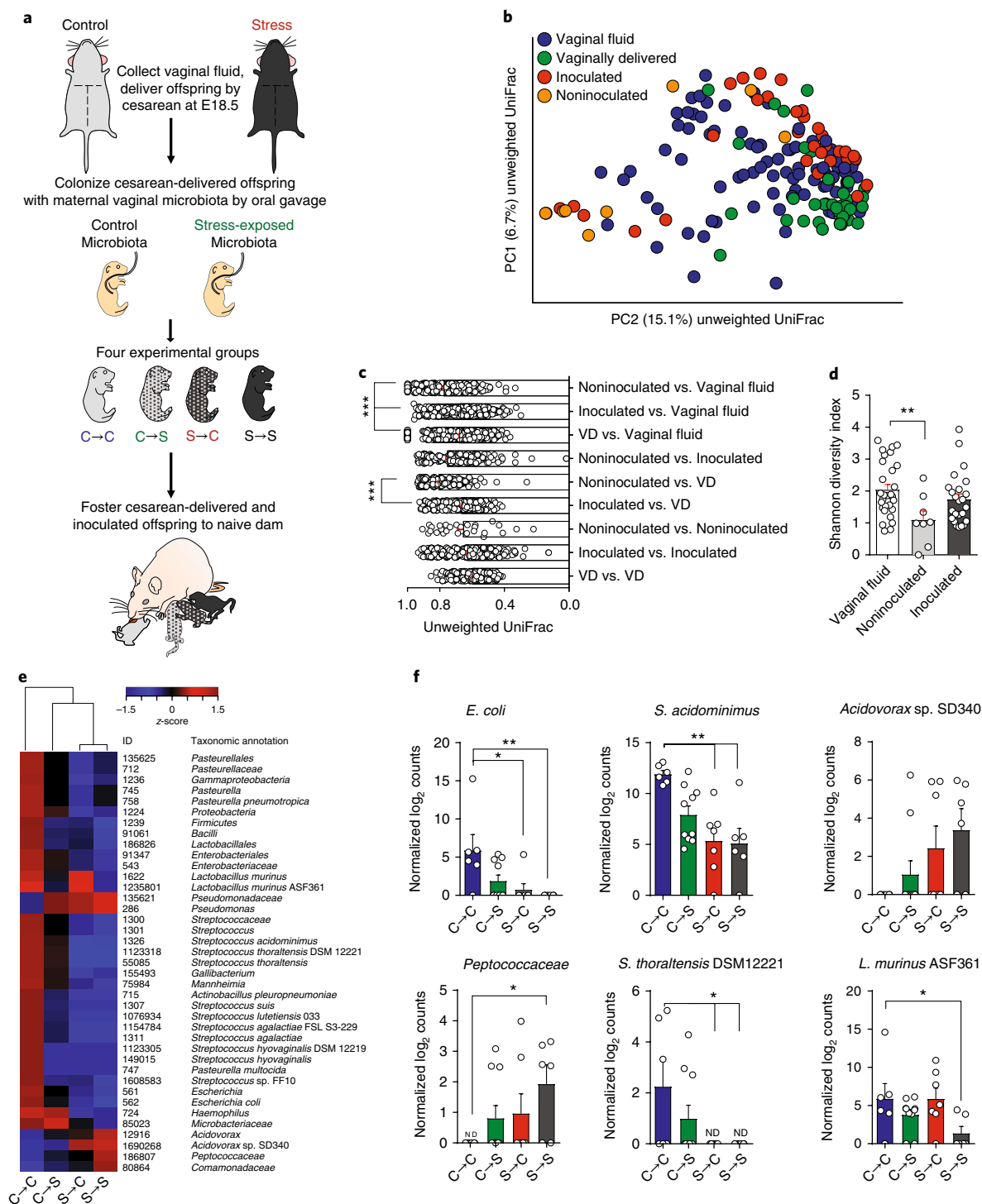
Following this validation, we next tested the hypothesis that the composition of the pioneer community of microbiota colonizing the neonate gut can be shaped by a vaginal fluid inoculant from control and stress-exposed dams. Control and prenatal-stress-exposed offspring were delivered by cesarean and gavaged with a vaginal inoculant from either control dams (i.e., microbiome from control dams transplanted into control offspring, C→C; or microbiome from control dams transplanted into stress-exposed offspring, C→S) or stress-exposed dams (i.e., microbiome from stress-exposed dams transferred into control offspring, S→C; or microbiome from stress-exposed dams transferred into stress-exposed offspring, S→S; Fig. 1a). Using a 16S rRNA marker gene sequencing approach, we compared gut microbiota parameters between vaginally delivered offspring and cesarean-delivered groups (C→C, C→S, S→C, and S→S) at P2. Assessment of bacterial diversity (Shannon Diversity Index) and phylogenetic distance measures (unweighted UniFrac) revealed no differences between treatment groups (Supplementary Fig. 1b–d). Consistent with our previously reported differences between vaginally delivered control and prenatal-stress-exposed offspring<sup>10</sup>, we observed differences in the microbial community composition and abundance between C→C and S→S offspring. Specifically, we observed differences in the abundance of *Escherichia coli*, *Streptococcus acidominimus*, *Peptococcaceae*, and *Streptococcus thoralensis* between C→C and S→S offspring (Fig. 1e,f). Comparison of gut community composition between C→C, C→S, S→C, and S→S

offspring at P2 revealed no differences in *E. coli* and *S. acidominimus* abundance between C→C and C→S offspring and no differences in *E. coli*, *S. acidominimus*, *Peptococcaceae*, and *S. thoralensis* between S→C and S→S offspring (Fig. 1e,f). Further, we observed differences in the abundance of *E. coli*, *S. acidominimus*, and *S. thoralensis* between C→C and S→C offspring, revealing that colonizing control offspring with a vaginal inoculant from a stress-exposed dam resulted in a gut community composition that was not different from S→S offspring.

Of the microbiota colonizing the neonate gut, the genus *Lactobacillus* influences brain GABA-receptor expression and stress-induced corticosterone production and behavior<sup>20</sup>. Prenatal-stress-exposed offspring showed reduced gut lactobacilli abundance that was associated with altered free amino acid levels in the P2 hypothalamus<sup>11,20–23</sup>. As this genus encompasses species with metabolic and immunological properties important for normal neurodevelopment, we used a whole-metagenomic shotgun sequencing approach to gain species- and strain-level resolution of lactobacilli in the P2 colon<sup>24,25</sup>. We detected reads mapping to *L. murinus*, *L. johnsonii*, *L. animalis*, and *L. apodemi* in the P2 colon. *L. murinus* ASF361, a species that colonizes the intestinal epithelium and engages in pathogen barrier defense, was the species with greatest abundance in the P2 offspring colon<sup>26</sup> (Supplementary Fig. 2). *L. murinus* ASF361 abundance was significantly reduced in S→S compared with C→C male offspring, replicating our previous work<sup>10,11</sup> (Fig. 1f). However, the effect on *L. murinus* ASF361 was not rescued in C→S offspring and was not recapitulated in S→C offspring, suggesting that factors other than maternal microbiota influence which pioneer group of organisms colonize the neonate gut (Fig. 1f).

**Maternal vaginal microbiota mediate the effects of prenatal stress on body weight and stress response.** To assess whether the maternal vaginal microbiome mediates the effects of prenatal stress on the offspring, we compared C→C, C→S, S→C, and S→S male offspring during development and into adulthood. Body weight measurements from P14 to P70 showed that the body weight growth curve for S→S male offspring was lower than that of C→C male offspring, replicating our previously published results for the effects of

**Fig. 1 | Oral gavage with vaginal microbiota from parturient stressed dams modulates offspring gut colonization patterns.** **a**, Schematic of the method we developed to manipulate the colonizing microbiome in conventionally housed mice. **b**, Vaginal microbiota transplantation recapitulates early life gut colonization patterns. Communities clustered using PCA of the unweighted UniFrac distance matrix, where each point corresponds to a sample collected from maternal vaginal fluid (blue), P2 colons of vaginally delivered offspring (green), P2 colons of cesarean-delivered and inoculated offspring (red), and P2 colons of cesarean-delivered and noninoculated offspring (orange). The percentage of variation explained by the principal coordinate is indicated on the axes ( $n = 8$  cesarean-delivered noninoculated mice;  $n = 24$  cesarean-delivered inoculated mice;  $n = 29$  vaginally delivered mice,  $n = 29$  maternal vaginal samples). PC, principal coordinate; PCA, principal coordinate analysis. **c**, Inoculation with maternal vaginal microbiota recapitulates community structure of vaginally delivered offspring. Average ( $\pm$  s.e.m.) unweighted UniFrac distances comparing phylogenetic configurations of bacterial communities from maternal vaginal fluid, P2 colons of vaginal delivered offspring, P2 colons of cesarean delivered and inoculated offspring, and P2 colons of noninoculated cesarean delivered offspring ( $n = 8$  cesarean-delivered noninoculated colons;  $n = 24$  cesarean-delivered inoculated colons;  $n = 29$  vaginally delivered colons,  $n = 29$  maternal vaginal samples;  $***P < 0.001$ , two-sided Mann-Whitney  $U$  test). Data represented as mean  $\pm$  s.e.m. with individual UniFrac distance correlations overlaid. VD, Vaginally delivered. **d**, Inoculation with maternal vaginal microbiota recapitulates community diversity of vaginally delivered offspring. Comparison of Shannon Diversity Index from P2 colons of vaginally delivered offspring, P2 colons of cesarean-delivered and inoculated offspring, and P2 colons of cesarean-delivered and noninoculated offspring demonstrating a significant decrease in community diversity in noninoculated cesarean-delivered offspring ( $P = 0.0078$ ), which was rescued in cesarean-delivered and inoculated offspring ( $n = 8$  cesarean-delivered noninoculated colons;  $n = 24$  cesarean-delivered inoculated colons;  $n = 29$  vaginally delivered colons;  $**P < 0.01$ , two-sided Mann-Whitney  $U$  test). Data presented as mean  $\pm$  s.e.m. with individual data points overlaid. **e**, Heat map depicting unsupervised clustering of samples (columns) from whole-metagenomic shotgun analyses demonstrating recapitulation of colonization patterns at bacterial-strain resolution (linear fit model, statistical parameters:  $P < 0.01$ ,  $\log(\text{FC}) > 2.0$ ). The taxonomic annotation of each taxa is indicated to the right of rows ( $n = 6$  C→C males;  $n = 10$  C→S males;  $n = 7$  S→C males;  $n = 6$  S→S males). FC, fold change. **f**, Bar plots of strain-resolved bacteria demonstrating that colonization patterns in S→C and C→S offspring were mediated by the maternal vaginal inoculant ( $n = 6$  C→C males;  $n = 10$  C→S males;  $n = 7$  S→C males;  $n = 6$  S→S males. *E. coli*, one-way ANOVA,  $F_{3,25} = 5.033$ ,  $P = 0.0073$ ; two-sided Fisher's LSD post hoc test, C→C vs. S→S,  $t_{25} = 5.003$ ,  $P = 0.0082$ ; C→C vs. S→C,  $t_{25} = 4.519$ ,  $P = 0.0184$ ; *S. acidominimus*, one-way ANOVA,  $F_{3,25} = 7.708$ ,  $P = 0.0008$ , two-sided Fisher's LSD post hoc test, C→C vs. S→S,  $t_{25} = 5.893$ ,  $P = 0.0017$ ; C→C vs. S→C,  $t_{25} = 5.891$ ,  $P = 0.0017$ ; *Peptococcaceae*, C→C vs. S→S,  $t_{25} = 2.515$ ,  $P = 0.0187$ ; *L. murinus*,  $t_{25} = 2.413$ ,  $P = 0.0235$ ; *S. thoralensis*, one-way ANOVA,  $F_{3,25} = 3.116$ ,  $P = 0.0441$ ; two-sided Fisher's least significant difference (LSD) post hoc test, C→C vs. S→S,  $t_{25} = 2.581$ ,  $P = 0.0161$ ; C→C vs. S→C,  $t_{25} = 2.678$ ,  $P = 0.0129$ ).  $*P < 0.05$ ,  $**P < 0.01$ . Data represented as mean  $\pm$  s.e.m. with individual data points overlaid. Sp., species.



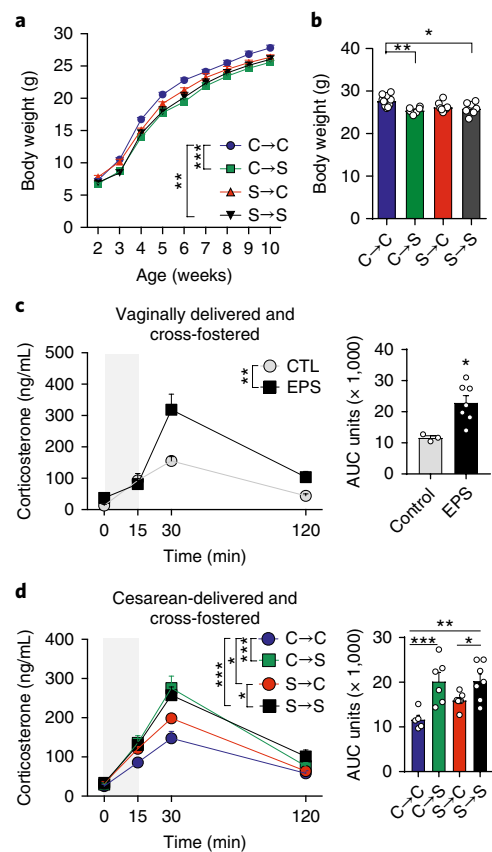
maternal stress<sup>13,16,27</sup> (Fig. 2a). The body weight growth curve of C→S males was reduced compared with C→C males, while no differences were detected in body weights between C→S and S→S males, indicating no rescue of the prenatal-stress body weight phenotype in prenatal-stress-exposed males inoculated with microbiota from control dams (Fig. 2a). Notably, the body weight of S→C males was not significantly different from either C→C or S→S males, showing an intermediate body weight phenotype in S→C males inoculated with microbiota from stress-exposed dams (Fig. 2a). Comparisons of final adult body weights at P70 revealed a significantly lower body weight for S→S males compared with C→C males (Fig. 2b). However, no significant difference was observed between S→C and

S→S males, again indicating an intermediate body weight in S→C males (Fig. 2b). Consistent with previous male-specific effects of prenatal stress in our model<sup>15</sup>, no differences in body weight measurements were observed between the four groups in female offspring (data not shown).

To examine the hypothalamic–pituitary–adrenal axis stress response, we measured plasma corticosterone levels following a 15-min restraint stress in adult offspring. We first assessed the effect of prenatal stress in vaginally delivered, cross-fostered offspring. This revealed that acute stress-induced corticosterone levels were significantly higher in prenatally stressed males compared with control male offspring (Fig. 2c), whereas there was no effect of prenatal stress

**Fig. 2 | The maternal vaginal microbiome partially mediates effects of prenatal stress on offspring body weight and corticosterone stress responses.**

**a.** Body weight was significantly changed over time (two-way ANOVA, main effect of time,  $F_{8,216} = 3,609$ ,  $P < 0.0001$ ), across treatment (two-way ANOVA, main effect of treatment,  $F_{3,27} = 6.781$ ,  $P = 0.0015$ ) and their interaction (two-way ANOVA, time  $\times$  treatment interaction,  $F_{24,216} = 3.42$ ,  $P = 0.00000767$ ). Post hoc analysis revealed that S $\rightarrow$ S males weighed less than C $\rightarrow$ C males across development (two-sided Fisher's LSD,  $t_{27} = 3.492$ ,  $P = 0.0017$ ). Transmission of stress-altered maternal vaginal microbiota resulted in an intermediate growth pattern in S $\rightarrow$ C males relative to C $\rightarrow$ C males ( $t_{27} = 1.987$ ,  $P = 0.0571$ ), while body weight was not normalized in C $\rightarrow$ S males relative to S $\rightarrow$ S males ( $t_{27} = 0.604$ ,  $P = 0.5506$ ). Statistics reflect two-way ANOVA with time as repeated measure followed by two-sided Fisher's LSD post hoc analysis.  $**P < 0.01$ ,  $***P < 0.001$ . **b.** Comparison of adult body weight at P70 between treatment groups revealed differences in body weight (one-way ANOVA, main effect of treatment,  $F_{3,27} = 5.355$ ,  $P = 0.005$ ). Body weight of S $\rightarrow$ S males was lower than in C $\rightarrow$ C males ( $t_{27} = 2.981$ ,  $P = 0.0289$ ). No difference in P70 body weight was observed between S $\rightarrow$ C and S $\rightarrow$ S males ( $t_{27} = 0.7242$ ,  $P = 0.955$ ), indicating an intermediate body weight phenotype in S $\rightarrow$ C males. C $\rightarrow$ S males also weighed less than C $\rightarrow$ C males at P70 ( $t_{27} = 5.028$ ,  $P = 0.0073$ ), indicating that transplantation of control maternal microbiota did not rescue this aspect of the prenatal stress phenotype. One-way ANOVA followed by two-sided Tukey's post hoc analysis;  $n = 10$  C $\rightarrow$ C males;  $n = 6$  C $\rightarrow$ S males;  $n = 8$  S $\rightarrow$ C males;  $n = 7$  S $\rightarrow$ S males in **a** and **b**.  $*P < 0.05$ ,  $**P < 0.01$ ,  $***P < 0.001$ . **c.** Left: vaginally delivered, cross-fostered prenatal-stress-exposed male offspring have higher stress-induced plasma corticosterone levels than vaginally delivered control offspring (two-way ANOVA, main effect of time,  $F_{3,24} = 14.26$ ,  $P = 0.0000152$ ; main effect of treatment,  $F_{1,8} = 14.19$ ,  $P = 0.0055$ ;  $n = 3$  control males;  $n = 7$  prenatal-stress-exposed males); stress duration is indicated by the shaded column. Right: total AUC corticosterone levels differed between experimental groups (unpaired two-sided  $t$  test,  $t_8 = 3.077$ ,  $P = 0.015$ ;  $n = 3$  control males;  $n = 7$  prenatal-stress-exposed males). EPS, early prenatal stress; AUC, area under curve.  $*P < 0.05$ . **d.** Left: corticosterone levels over time were different across treatment groups (main effect of time,  $F_{3,63} = 176.7$ ,  $P < 0.0001$ ; main effect of experimental group,  $F_{3,21} = 8.393$ ,  $P = 0.0007$ ; time  $\times$  group interaction,  $F_{9,63} = 3.962$ ,  $P = 0.0005$ ). S $\rightarrow$ S males had higher corticosterone levels over time than C $\rightarrow$ C males (two-sided Fisher's LSD post hoc analysis;  $t_{21} = 4.398$ ,  $P = 0.0003$ ) and S $\rightarrow$ C males ( $t_{21} = 2.506$ ,  $P = 0.0205$ ). S $\rightarrow$ C males had higher corticosterone levels than C $\rightarrow$ C offspring ( $t_{21} = 2.11$ ,  $P = 0.0470$ ), demonstrating an intermediate phenotype of corticosterone response in S $\rightarrow$ C males. Analysis of peak (30 min) corticosterone levels showed that S $\rightarrow$ S males had higher peak corticosterone levels than C $\rightarrow$ C ( $t_{84} = 8.054$ ,  $P < 0.0001$ ) and S $\rightarrow$ C males ( $t_{84} = 4.727$ ,  $P = 0.00067$ ). S $\rightarrow$ C males had higher peak corticosterone levels compared with C $\rightarrow$ C males ( $t_{84} = 3.739$ ,  $P = 0.0472$ ), indicating an intermediate peak corticosterone response following an acute restraint stress. Corticosterone levels over time and at the peak were similar in C $\rightarrow$ S offspring and S $\rightarrow$ S offspring (over time,  $t_{21} = 0.126$ ,  $P = 0.9003$ ; peak,  $t_{84} = 1.393$ ,  $P = 0.7585$ ), indicating that transplantation of control microbiota did not rescue this aspect of the prenatal stress phenotype in males. Two-way ANOVA with time as a repeated measure followed by two-sided Fisher's LSD post hoc analysis;  $n = 5$  C $\rightarrow$ C males;  $n = 6$  C $\rightarrow$ S males;  $n = 7$  S $\rightarrow$ C males;  $n = 7$  S $\rightarrow$ S males.  $*P < 0.05$ ,  $***P < 0.001$ . Right: total AUC of corticosterone levels differed between experimental groups (one-way ANOVA; group,  $F_{3,21} = 7.175$ ,  $P = 0.0017$ ; two-sided Fisher's LSD post hoc analysis; C $\rightarrow$ C vs. S $\rightarrow$ S,  $t_{21} = 3.632$ ,  $P = 0.0016$ ; C $\rightarrow$ C vs. C $\rightarrow$ S,  $t_{21} = 4.089$ ,  $P = 0.0005$ ; S $\rightarrow$ C vs. S $\rightarrow$ S,  $t_{21} = 2.131$ ,  $P = 0.045$ ;  $n = 5$  C $\rightarrow$ C males;  $n = 6$  C $\rightarrow$ S males;  $n = 7$  S $\rightarrow$ C males;  $n = 7$  S $\rightarrow$ S males). For hypothalamic-pituitary-adrenal stress axis experiments, results shown are representative of two independent experimental replicates,  $*P < 0.05$ ,  $**P < 0.01$ ,  $***P < 0.001$ . Data represented as mean  $\pm$  s.e.m. with individual data points overlaid.



on corticosterone levels female offspring (Supplementary Fig. 3). These data replicate our previous findings in non-cross-fostered offspring<sup>12–16</sup>.

We next examined the role of the maternal vaginal microbiota in this prenatal-stress effect in male C $\rightarrow$ C, C $\rightarrow$ S, S $\rightarrow$ C, and S $\rightarrow$ S adult offspring. Stress-induced corticosterone levels were significantly higher in male S $\rightarrow$ S offspring compared with C $\rightarrow$ C offspring (Fig. 2d), again replicating the effect of prenatal stress in our previous studies<sup>12–16</sup>. Corticosterone levels in response to restraint in male S $\rightarrow$ C offspring were increased compared with C $\rightarrow$ C offspring (Fig. 2d), but were not significantly different from those of S $\rightarrow$ S males, again suggesting an intermediate phenotype and a possible mediating effect of the maternal vaginal microbiome on this aspect of the prenatal stress phenotype. Male C $\rightarrow$ S offspring had a stress response that was higher than C $\rightarrow$ C offspring and that did not significantly differ from S $\rightarrow$ S offspring (Fig. 2d), suggesting that transplantation of a control maternal vaginal microbiome was not able to rescue this aspect of the prenatal stress phenotype. We also assessed the peak (30 min) of the corticosterone response, as this timepoint is the typical maximal rise of the stress response. We found that peak corticosterone levels were significantly increased in male S $\rightarrow$ C offspring compared with C $\rightarrow$ C offspring, but peak corticosterone levels in S $\rightarrow$ S males remained higher than S $\rightarrow$ C males (Fig. 2d), further suggesting an intermediate prenatal stress phenotype in control offspring colonized by vaginal microbiota from stress-exposed dams.

In addition, we assessed whether cesarean delivery and inoculation with maternal vaginal microbiota or in cross-fostering would impact corticosterone response to acute stress in females. Consistent with previous male-specific effects of prenatal stress in our model<sup>15</sup>, we observed no differences in corticosterone levels between the four treatment groups in female offspring (Supplementary Fig. 3). In addition, there was no effect of prenatal stress on locomotor activity or anxiety-like behaviors in the light–dark box in either male or

female offspring, confirming our previous studies<sup>15</sup>, nor was there an effect of cesarean delivery and inoculation with maternal vaginal microbiota or cross-fostering in this test (Supplementary Fig. 4).

**Prenatal stress induces changes in the fetal intestinal niche in male offspring.** The host intestinal niche and mucosal immune system impose selective pressures upon bacterial communities in the adult gut<sup>28</sup>, but it is unclear whether or not the fetal intestinal niche also shapes the composition of the pioneer communities that colonize the offspring gut at birth. As inoculation with a control maternal vaginal microbiome could not rescue several aspects of the prenatal stress phenotype in male offspring, including reduced body weight and increased stress-induced corticosterone levels, we hypothesized that the fetal intestinal niche could itself be altered by prenatal stress; if so, this could subsequently contribute to changes in the postnatal microbiota composition and, thereby, to adult phenotypes. We conducted RNA-sequencing analyses of E18.5 fetal intestines from control and prenatal-stress-exposed males and females. Differential expression analyses ( $P < 0.01$ ,  $\log(\text{fold change}) = 1.5$ ) comparing fetal intestinal transcriptomes of male and female offspring revealed sexually dimorphic gene-expression patterns that were disrupted by prenatal stress (Supplementary Fig. 5), consistent with previous studies that have reported disruption of sex differences by prenatal stress<sup>12–16</sup>.

Comparisons of intestinal transcriptomes between control and prenatal-stress-exposed males revealed that the expression of transcripts for proteins involved in normal gastrointestinal development (*Gbx2*, *Adnp*), energy balance (*Rdh9*), and immune function (*Slamf7*, *Defa-rs7*, *Raet1e*, *Ceacam2*) were altered by prenatal stress (Fig. 3a,b). Gene-set enrichment analysis (GSEA) revealed enrichment of curated (C2) gene sets involved in immune function, and the expression of genes within these gene sets were increased in prenatal-stress-exposed males (Fig. 3c,d). Analysis of prenatal-stress-altered leading-edge subsets—designated as the gene set members accounting for the enrichment—included genes that play a role in innate immunity and inflammation, including those coding for myeloid differentiation primary response 88 (*MyD88*), interleukin-1 receptor-associated kinase 1 (*Irak1*), and TNF receptor-associated factor 6 (*Traf6*; Supplementary Tables 1 and 2). As these genes are involved in downstream signaling events that induce transcription of inflammatory cytokines, we measured expression levels of the proinflammatory cytokine, tumor necrosis factor- $\alpha$  (TNF $\alpha$ )<sup>29</sup> in the intestine. TNF $\alpha$  was higher in E18.5 male prenatal-stress-exposed fetuses relative to control males, suggesting that prenatal stress may induce intestinal inflammation in males even before microbial colonization (Supplementary Fig. 5e). No gene sets were significantly different for female prenatal stress and control groups (all false-discovery rate (FDR) values  $> 0.25$ ; data not shown).

As genes within the male enriched gene sets were also involved in the recruitment of immune cells to local tissues, we assessed whether immune cell populations present in the fetal intestine differed between prenatal stress and control groups. Specifically, we determined the effect of prenatal stress on myeloid populations<sup>30,31</sup>, as these are an essential component of the innate immune system that supports intestinal colonization and containment of complex microbiota. Multicolor flow cytometry analysis identified an increase in the frequency of CD45<sup>+</sup>CD11b<sup>+</sup>Ly6G<sup>+</sup>Ly6C<sup>+</sup> inflammatory monocytes in the E18.5 fetal intestine of prenatal-stress-exposed males relative to controls (Fig. 3e,f), consistent with the proinflammatory phenotype revealed by our transcriptomic analyses. In addition, the frequency of CD45<sup>+</sup>CD11b<sup>+</sup>Ly6G<sup>+</sup> neutrophils was higher in the intestine of control female fetuses compared with male fetuses, and this sex difference was disrupted by prenatal stress (Fig. 3g,h).

We next assessed whether these differences in the fetal intestine were associated with differences in peripheral immunity measures

into adulthood. We used a ‘second-hit’ protocol in which adult control and prenatal-stress-exposed male mice were or were not exposed to one week of chronic variable stress, after which frequencies of splenic Ly6C<sup>+</sup> and Ly6C<sup>hi</sup> monocyte populations were examined. Stress exposure did not significantly increase the frequency of CD45<sup>+</sup>CD11b<sup>+</sup>Ly6G<sup>+</sup>Ly6C<sup>+</sup> inflammatory monocytes in the spleen of prenatal-stress-exposed male mice relative to controls ( $P = 0.0616$ ; Supplementary Fig. 6). In addition, TNF $\alpha$  levels were not significantly increased in splenic CD11b<sup>+</sup>Ly6C<sup>+</sup> monocytes in prenatal-stress-exposed males relative to controls ( $P = 0.0554$ ; Supplementary Fig. 6).

### Chronic stress in adulthood unmasks effects of early prenatal stress on the gut.

Following colonization, the bacterial communities within the offspring gut undergo dynamic restructuring that involves complex gene–environment interactions<sup>32</sup>. We have previously shown that prenatal stress exposure has lasting effects on the assembly and maturation patterns of the gut microbiota and that these changes precede the emergence of aspects of the prenatal stress phenotype in male offspring<sup>10</sup>. Taken together with our observations that prenatal stress exposure influences the intestinal niche, this raises the possibility that enduring changes to host–microbe interactions increases the sensitivity of male offspring to effects of additional stresses later in life. To examine this possibility, we again used the second-hit protocol in which adult C→C, C→S, S→C, and S→S male offspring were or were not exposed to chronic variable stress for one week. We subsequently quantified intestinal permeability by measuring the translocation of fluorescein isothiocyanate (FITC)-dextran across the intestinal epithelium and into circulation<sup>33</sup>. While no baseline differences were detected in intestinal permeability between the four treatment groups (Fig. 4a), following chronic stress, intestinal permeability in all treatment groups was significantly different from that in groups that were not exposed to chronic stress. In addition, S→S males exposed to additional stress in adulthood showed significantly increased intestinal permeability compared with C→C males exposed to stress in adulthood (Fig. 4a).

We next examined how chronic variable stress in adulthood influences gut microbiota community composition in C→C, C→S, S→C, and S→S males by comparing strain-resolved shotgun data from fecal samples collected from mice with or without chronic stress exposure (Fig. 4b). At the community level, microbiota analysis by principal coordinates analysis with multidimensional scaling showed that the two stress sample sets formed distinct communities and that complex interactions existed for adult stress and treatment group (Fig. 4b). To further examine these interactions, we used a rank–rank hypergeometric overlap test (Fig. 4c). We observed that taxa enriched in S→S males without stress exposure (versus unstressed C→C males) were also enriched in S→S males exposed to chronic stress relative to chronically stressed C→C males ( $\max \log_{10}(P) = 3$ ), indicating that differences in community composition were maintained regardless of stress exposure in adulthood in S→S males. In addition, we identified taxa that were enriched in S→S without stress exposure relative to C→C males and that were depleted in S→S males exposed to chronic stress ( $\max \log_{10}(P) = 3$ ), showing taxa that were sensitive to disruption by chronic stress in S→S males. S→C males exhibited an enrichment of taxa regardless of chronic stress exposure in adulthood relative to C→C males, as well as taxa that were enriched in S→C males without chronic stress and depleted in chronically stressed S→C males ( $\max \log_{10}(P) = 3$ ). The similar patterns of depletion of taxa in S→C and S→S males relative to C→C males following chronic stress exposure may suggest a role of the maternal vaginal microbiome in mediating effects of adulthood stress on taxa. In contrast, we only observed enrichment of taxa in C→S relative to C→C independent of stress exposure ( $\max \log_{10}(P) = 8$ ), suggesting similar effects of chronic stress exposure on community composition between C→S and C→C males.

Using this approach, we identified two bacterial species altered by adult stress exposure. *Staphylococcus lentus*, a species reported to induce transcription of host pro-inflammatory genes, was increased in abundance in all four treatment groups following chronic stress exposure (Fig. 4d). S→S males compared to C→C and S→C males showed increased abundance of *S. lentus* only if they had undergone chronic stress in adulthood (Fig. 4d)<sup>34,35</sup>. *S. lentus* counts did not differ between chronically stressed C→S and S→S males, further demonstrating a failure of the maternal vaginal microbiome to rescue the effects of prenatal stress. By contrast, *Lactobacillus reuteri*, a species involved in maintaining intestinal barrier function, was more abundant in unstressed S→S males than in C→C males; however, this difference was not observed between chronically stressed S→S and C→C males (Fig. 4e)<sup>36</sup>. Chronic stress-induced alterations to *L. reuteri* were neither rescued in C→S males nor recapitulated in S→C males (Fig. 4e). Taken together, these analyses reveal gut microbiota that were both sensitive and resistant to adult stress exposure, and they highlight the possibility that the maternal vaginal microbiome may mediate some effect of stress exposure on gut microbiota in adult males.

**Prenatal stress is associated with altered gene expression in the PVN of males exposed to adulthood stress.** We previously demonstrated an association between the gut microbiota and amino acid availability in the hypothalamus on P2<sup>11</sup>. To examine whether early-life experience may interact with adulthood stress (possibly via effects on the gut microbiota) to influence the hypothalamus, we compared transcriptional profiles, using RNA-seq, of C→C, C→S, S→C, and S→S males exposed to chronic stress. GSEA revealed enrichment of curated C2 gene sets for neurotrophin signaling and energy metabolism in the paraventricular nucleus of the hypothalamus (PVN) in C→C males versus S→S males, indicating that the expression of member genes was disrupted in S→S males that had undergone stress as adults (Fig. 5a–c and Supplementary Tables 3–5). Differential gene expression analysis ( $P < 0.01$ ,  $\log(\text{fold change}) > 2$ ) comparing adult stress-exposed C→C and S→S males identified 95 genes with altered expression in the PVN (Fig. 5d). Lastly, we assessed whether this difference was recapitulated in S→C males and/or rescued in C→S males. GSEA revealed no enrichment of gene sets in the S→C and C→S males relative to C→C or S→S males following adult stress. Comparisons of gene-expression patterns in the PVN of all four groups revealed that chronically stressed S→C and C→S males both exhibited an intermediate phenotype following stress exposure, with gene clusters sharing some overlap with both chronically stressed C→C and chronically stressed S→S males (Fig. 5d,e).

## Discussion

The transition from an intrauterine to postnatal environment involves colonization by maternal vaginal microbiota that stimulate immune and metabolic processes in the offspring. Epidemiological studies have reported associations between cesarean delivery and increased risk for obesity, asthma, and allergies, suggesting that exposure to vaginal microbiota during birth may be linked to long-term health outcomes. Given that a limited consortium of bacteria colonizes the neonate gut, shifts in the composition of this pioneer community may have lasting effects on offspring. Using our mouse model of early prenatal stress, we previously demonstrated that exposure to stress during the first week of pregnancy resulted in lasting disruption to the maternal vaginal microbiome and altered the composition of bacteria colonizing the neonate gut at birth and that this was associated with altered metabolite profiles in the neonatal gut and hypothalamus at P2<sup>11</sup>. This suggested, but did not prove, that prenatal-stress-associated changes in the offspring gut microbiota may mediate the effects of prenatal stress on offspring gut and hypothalamus.

To investigate the causal contribution of the maternal vaginal microbiota to the effects of prenatal stress on the offspring, we used cesarean delivery at E18.5 to prevent colonization, and then applied oral gavage of vaginal inoculant from either control or stress-exposed dams to the neonates. We demonstrated that the effects of maternal stress (S→S) on abundance of specific bacterial species in the offspring gut—*E. coli*, *S. acidominimus*, and *Peptococcaceae*—were recapitulated in S→C offspring. These facultative anaerobic species colonize the neonate gut, regulate mucosal immunity, and metabolically prime the intestinal niche for replacement by other anaerobic bacteria that produce metabolites important for neurodevelopment<sup>37</sup>. Previous work in rodent<sup>10,11</sup> and primate<sup>38,39</sup> models of prenatal stress have reported reduced abundance of *Lactobacillus* in the gut of stress-exposed offspring and an association with altered availability of amino acids in the P2 gut and hypothalamus. We identified *L. murinus* ASF361 as the most abundant *Lactobacillus* species in the P2 gut. However, inoculation with vaginal microbiota from control or stress-exposed dams showed neither recapitulation (i.e., S→C offspring) nor rescue (i.e., C→S offspring) of *L. murinus* ASF361 abundance, suggesting that gestational factors, such as the impact of maternal antibodies or metabolites on the fetal gut<sup>40</sup>, may influence the ability of certain bacterial species to successfully colonize the gut at birth and into the early postnatal window. In adulthood, the maternal vaginal microbiome showed a mediating effect on key aspects of the prenatal stress phenotype. Control male offspring transplanted with a vaginal inoculant from stress-exposed dams (i.e., S→C offspring) exhibited an intermediate body weight curve and intermediate corticosterone levels following exposure to acute stress. However, prenatal-stress-exposed offspring transplanted with a vaginal inoculant from control dams (C→S) did not show a rescue of prenatal stress effects on body weight and corticosterone response to acute stress. These results demonstrate that prenatal insults such as maternal stress have effects on offspring that are partially mediated by the maternal vaginal microbiota, but that cannot be rescued by it.

The inability of maternal control microbiota transfer (i.e., in C→S offspring) to fully rescue the prenatal stress phenotype suggests that the prenatal environment has a direct effect on the gut during prenatal development. RNA-seq analysis on E18.5 intestines from control and prenatal-stress-exposed male and female offspring revealed enrichment of innate immunity and interferon-response gene sets in prenatally stressed males, reflecting an increased expression of these genes in the fetal intestine of prenatally stress-exposed males, but not females. Prenatal stress exposure may also increase levels of intestinal inflammation, as pro-inflammatory cytokine transcript levels and frequency of inflammatory monocytes were increased in prenatal-stress-exposed males. A role for the maternal gut microbiome on offspring immune system development has been recently demonstrated<sup>40</sup>, highlighting the possibility that maternal gut microbial changes in response to stress may also contribute to the observed alterations in offspring immunity<sup>40</sup>. In previous work, we exposed pregnant dams to stress and longitudinally determined the composition of their gut microbiota to assess whether stress impacted pregnancy-associated shifts in the maternal gut microbiota<sup>10</sup>. Chronic stress during the first week of pregnancy disrupted pregnancy-associated shifts<sup>10</sup>, characterized by enrichment of taxa associated with intestinal inflammation and by disruption to putative microbial pathways involved in amino acid and fatty acid metabolism<sup>10</sup>. The association between stress-induced changes to the maternal gut microbiota and prenatal stress effects on the fetal intestinal niche may suggest a role for the maternal gut microbiome on fetal immunity<sup>41</sup>, but more work will be needed to examine causality.

The fetal intestine inflammatory response in prenatally stressed males may also reduce the availability of nutrients and substrates within the gut lumen that support growth of both fetal tissue and

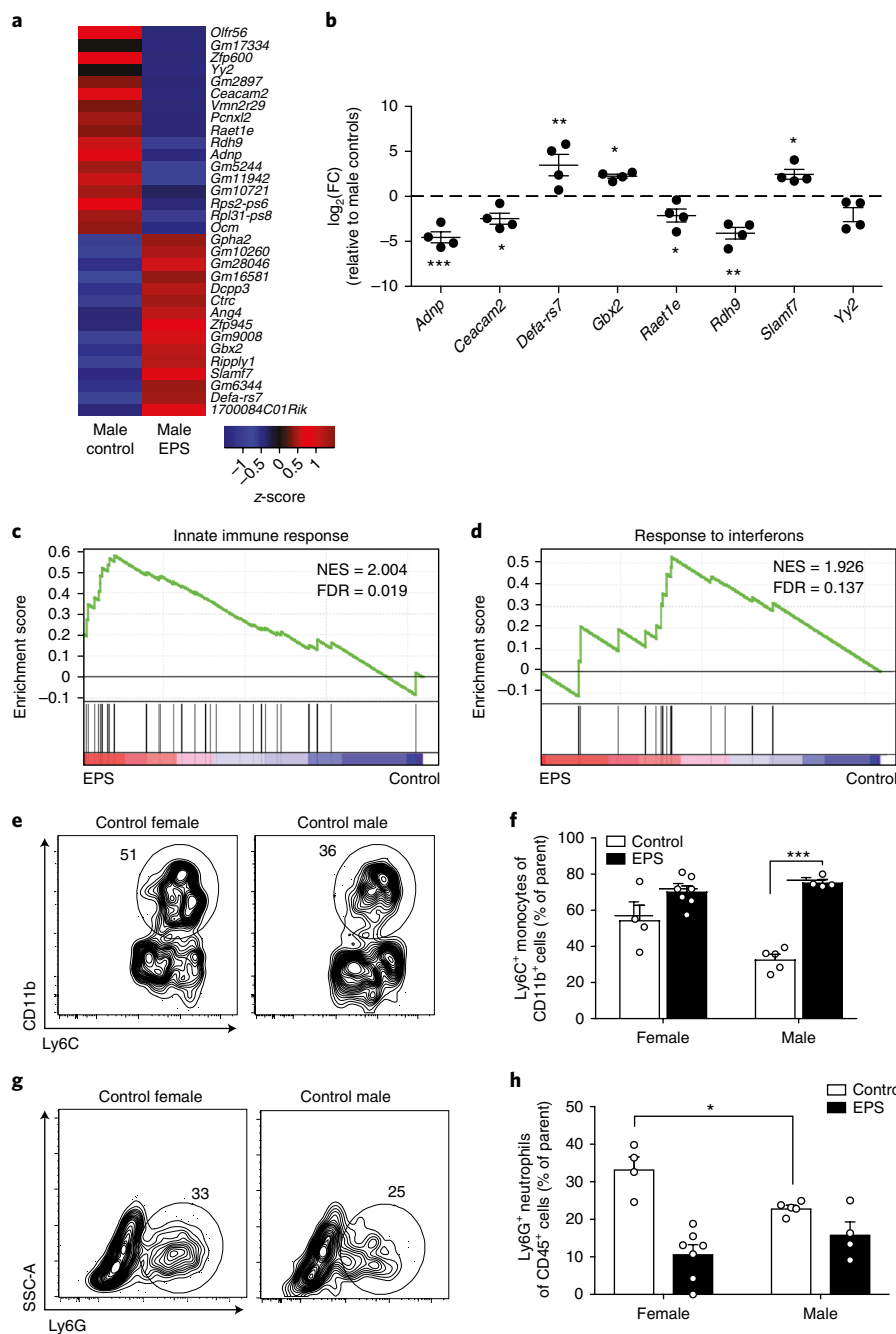


**Fig. 3 | Early prenatal stress induces alterations in the fetal intestinal transcriptome and fetal intestinal immune cells in males. a**, Heatmap depicting mean expression of E18.5 fetal intestinal genes, showing differences between control males and EPS males (linear fit model,  $P < 0.01$ ,  $\log_2(\text{FC}) = 1.5$ ). **b**,  $\log_2(\text{FC})$  of selected fetal intestine genes shown to be involved in gastrointestinal development, energy balance, and immune function were differentially expressed in EPS males relative to control males. \* $P < 0.05$ , \*\* $P < 0.01$ , \*\*\* $P < 0.001$ ; unpaired two-sided  $t$  test. **c, d**, GSEA of RNA-seq data identified significant enrichment of gene sets in EPS males compared to control males (normalized enrichment score (NES)  $> 1.8$  and false discovery rate (FDR)  $< 0.25$ ; FDR = 0.019 for innate immune response; FDR = 0.137 for response to interferons), specifically for gene sets involved in the innate immune response and in the response to interferons. **e**, Representative flow cytometry contour plots showing gating of CD45<sup>+</sup>CD11b<sup>+</sup>Ly6G<sup>-</sup>Ly6C<sup>+</sup> cells and the percentage of Ly6C<sup>+</sup> (circle) cells from the E18.5 intestines of control and prenatal-stress-exposed males and females. **f**, Analysis of CD45<sup>+</sup>CD11b<sup>+</sup>Ly6G<sup>-</sup>Ly6C<sup>+</sup> monocytes in the E18.5 intestine (two-way ANOVA with two-sided Fisher's LSD, main effect of treatment,  $F_{1,16} = 47.64$ ,  $P = 0.00000355$ ; sex  $\times$  treatment interaction,  $F_{1,16} = 10$ ,  $P = 0.006$ ; Fisher's LSD post hoc analysis comparing male control vs. prenatal stress,  $t_{16} = 6.88$ ,  $P = 0.00000365$ ). \*\*\* $P < 0.01$ . Results shown are representative of two independent experimental replicates. Data represented as mean  $\pm$  s.e.m. with individual data points overlaid. **g**, Representative flow cytometry contour plots showing gating of CD45<sup>+</sup>CD11b<sup>+</sup>Ly6G<sup>+</sup> cells and the percentage of Ly6G<sup>+</sup> (circle) cells from the E18.5 intestines of control and prenatal-stress-exposed males and females. **h**, Analysis of CD45<sup>+</sup>CD11b<sup>+</sup>Ly6G<sup>+</sup> neutrophils in the E18.5 intestine revealed significant sex differences in control offspring that are disrupted by EPS (two-way ANOVA with two-sided Fisher's LSD, main effect of treatment,  $F_{1,16} = 31.31$ ,  $P = 0.0000402$ ; sex  $\times$  treatment interaction,  $F_{1,16} = 8.692$ ,  $P = 0.0094$ ; Fisher's LSD post hoc analysis comparing control male vs. control female,  $t_{16} = 2.69$ ,  $P = 0.0161$ ; female control vs. female EPS,  $t_{16} = 6.257$ ,  $P = 0.0000114$ ). \* $P < 0.05$ . Results shown are representative of two independent experimental replicates. Data represented as mean  $\pm$  s.e.m. with individual data points overlaid;  $n = 4$  control males;  $n = 4$  prenatal-stress-exposed males in panels **a-d**;  $n = 4$  control females;  $n = 7$  prenatal-stress-exposed females;  $n = 5$  control males;  $n = 4$  prenatal-stress-exposed males in **e-h**.

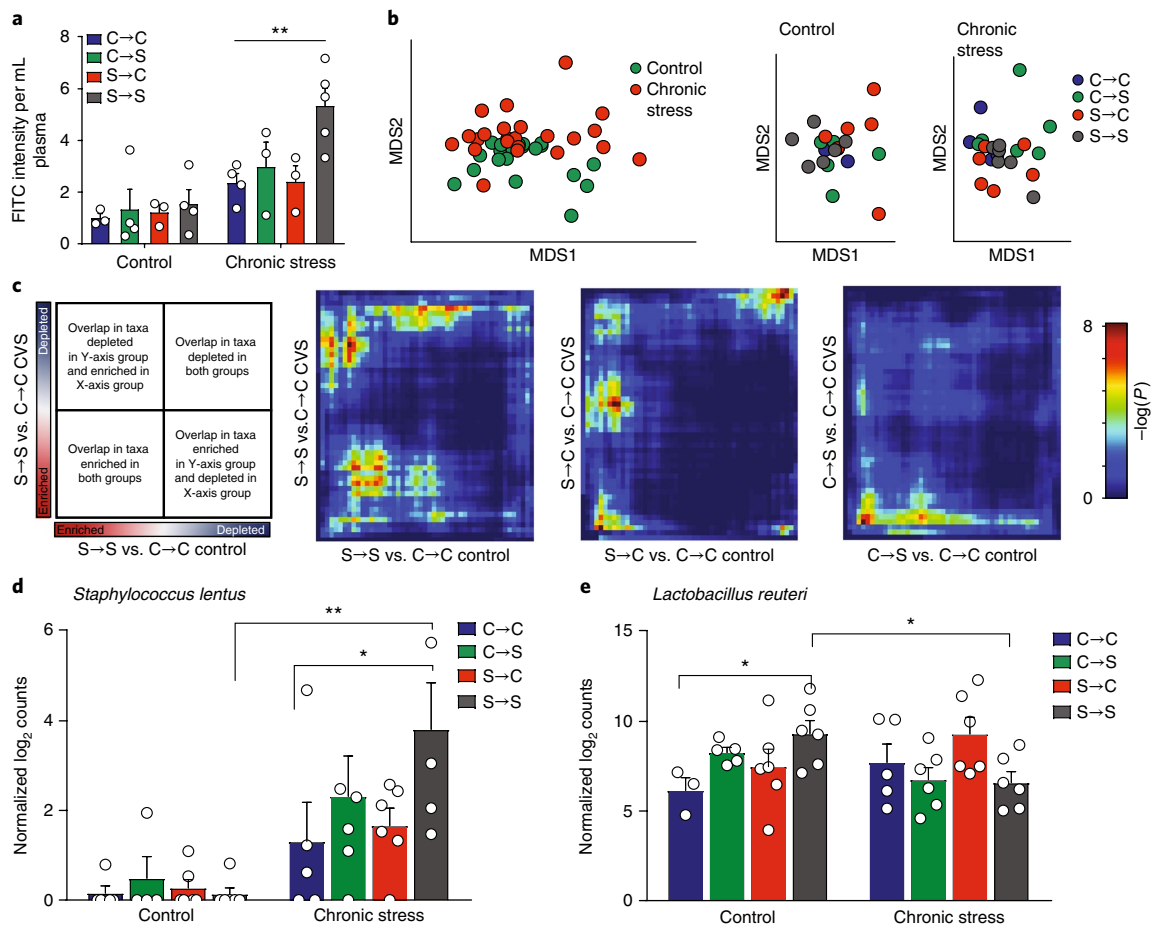


**Fig. 4 | Chronic stress in adulthood unmasks effects of early prenatal stress on intestinal permeability and gut microbiota. a**, Effects of early prenatal stress and chronic variable stress (CVS) exposure in adulthood on intestinal permeability in males (two-way ANOVA; main effect of prenatal stress exposure,  $F_{3,21} = 3.603$ ,  $P = 0.0304$ ; main effect of adult chronic stress exposure,  $F_{1,21} = 19.3$ ,  $P = 0.0003$ ). Post hoc analyses (two-sided Fisher's LSD) revealed that chronic stress-exposed S→S males had increased intestinal permeability compared with chronic stress-exposed C→C males ( $t_{21} = 3.697$ ,  $P = 0.008$ ). No differences in intestinal permeability were detected between the four treatment groups not exposed to chronic stress in adulthood (control; all  $P > 0.05$ ;  $n = 3$  control C→C males;  $n = 4$  control C→S males;  $n = 3$  control S→C males;  $n = 4$  control S→S males;  $n = 4$  chronic stress C→C males;  $n = 3$  chronic stress C→S males;  $n = 3$  chronic stress S→C males;  $n = 5$  chronic stress S→S males). Data represented relative to baseline control C→C males and data represented as mean  $\pm$  s.e.m. with individual data points overlaid. **b**, Communities clustered using MDS + PCA of the Bray-Curtis dissimilarity matrix, where each point corresponds to a fecal sample and demonstrates effects of chronic stress in adulthood on the gut microbial community structure. Left: community clustering comparing control (green circle) and post-chronic stress (red circle) for all samples demonstrating a separation of community structure between conditions. Middle: community clustering of control samples comparing C→C, C→S, S→C, and S→S males. Right: community clustering of post-chronic stress comparing C→C, C→S, S→C, and S→S males. Numbers of animals per group as in **b**. MDS, multidimensional scaling. **c**, Strain-resolved shotgun data for C→C, C→S, S→C, and S→S groups collected from control and post-CVS, showing the patterns and significance of overlap in microbiota communities between conditions by comparing threshold-free differential taxa abundance between control and post-chronic stress exposure. Each pixel represents taxa overlap between control and post-chronic stress exposure, with the significance of overlap ( $-\log_{10}(P)$  of a hypergeometric test; step size 200) color coded. The extent of overlap of enriched taxa is displayed in the bottom left, and the overlap of depleted taxa displayed in the top right, as illustrated in the left panel ( $n = 3$  control C→C males;  $n = 5$  control C→S males;  $n = 6$  control S→C males;  $n = 6$  control S→S males;  $n = 5$  post-chronic stress C→C males;  $n = 6$  post-chronic stress C→S males;  $n = 6$  post-chronic stress S→C males;  $n = 6$  post-chronic stress S→S males). **d**, Effect of chronic variable stress on *S. lentus* in C→C, C→S, S→C, and S→S males. Relative abundance of *S. lentus* showed a significant effect of chronic stress (two-way ANOVA with two-sided Fisher's LSD,  $F_{1,35} = 21.14$ ,  $P = 0.0000536$ ; post hoc analysis, control S→S vs. post-chronic stress S→S,  $t_{35} = 4.274$ ,  $P = 0.0001$ ; post-chronic stress C→C vs. post-chronic stress S→S,  $t_{35} = 2.791$ ,  $P = 0.0085$ ). Data represented as mean  $\pm$  s.e.m. \* $P < 0.05$ ; \*\* $P < 0.01$ . Numbers of animals per group as in **b**. **e**, Effect of chronic variable stress on *L. reuteri* in C→C, C→S, S→C, and S→S males. Relative abundance of *L. reuteri* showed a significant interaction between treatment group and chronic stress (two-way ANOVA with two-sided Fisher's LSD,  $F_{3,35} = 4.052$ ,  $P = 0.0142$ ; post hoc analysis, control S→S vs. post-chronic stress S→S,  $t_{35} = 2.556$ ,  $P = 0.0151$ ; control C→C vs. control stress S→S,  $t_{35} = 2.425$ ,  $P = 0.0206$ ). Data represented as mean  $\pm$  s.e.m. \* $P < 0.05$ . Numbers of animals per group as in **b**.

microbiota, as we have previously demonstrated that prenatal-stress-exposure decreased metabolite availability in the offspring colon at P21<sup>11,42</sup>. Prenatal-stress-induced intestinal inflammation and shifts in metabolite availability may represent negative selective forces that could explain the inability of control vaginal microbiome

inoculation to rescue (in C→S offspring) the altered colonization of lactobacilli seen in S→S offspring. Together, these data suggest that prenatal stress influences the fetal gut and that this may influence which pioneer bacterial communities to gain entry and establish residence.

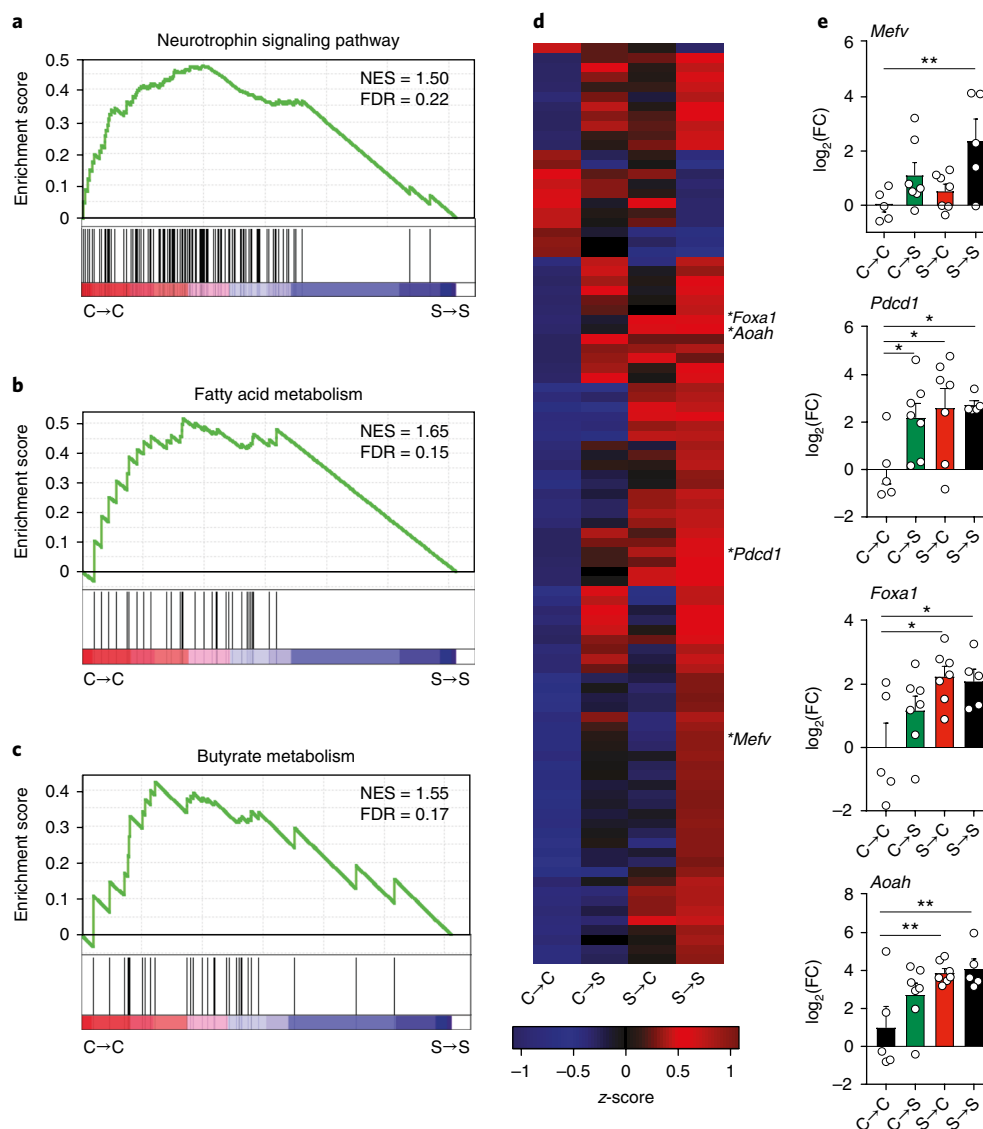


**Fig. 5 | Prenatal stress is associated with altered gene expression patterns in the PVN of males exposed to adulthood stress. a–c,** GSEA of RNA-seq results from the PVN of adult C→C and S→S males exposed to chronic variable stress. Three enriched curated gene sets with NES > 1.5 and FDR < 0.25 in C→C males exposed to chronic stress were altered relative to chronic stress exposed S→S males. **d,** Heatmap depicting mean expression of significantly altered PVN genes ( $P < 0.01$ ,  $\log_2(\text{FC}) > 2$ ). Differences between chronic stress-exposed C→C males and chronic stress-exposed S→S males were ameliorated in chronic stress-exposed S→C males and chronic stress-exposed C→S males, indicating that transplantation of the maternal vaginal microbiota has effects at the level of the PVN in adulthood. **e,** Select genes from differential gene expression analysis showing dysregulation in the PVN following chronic stress exposure in C→C, C→S, S→C, and S→S males. Gene expression of *Mefv*, *Pdc1*, *Aoah*, and *Foxa1* differed between the four treatment groups (main effect of treatment for *Mefv*,  $F_{3,20} = 4.194$ ,  $P = 0.0187$ ; main effect of treatment for *Pdc1*,  $F_{3,20} = 3.377$ ,  $P = 0.0386$ ; main effect of treatment for *Aoah*,  $F_{3,20} = 4.584$ ,  $P = 0.0134$ ; main effect of treatment for *Foxa1*,  $F_{3,20} = 4.269$ ,  $P = 0.0175$ ). Post hoc analysis (two-sided Fisher's LSD) showed that S→S males showed higher expression of *Mefv*, *Pdc1*, *Aoah*, and *Foxa1* than C→C males following chronic stress exposure (*Mefv*,  $t_{20} = 3.321$ ,  $P = 0.0034$ ; *Pdc1*,  $t_{20} = 2.724$ ,  $P = 0.0131$ ; *Aoah*,  $t_{20} = 3.313$ ,  $P = 0.0044$ ; *Foxa1*,  $t_{20} = 2.831$ ,  $P = 0.0103$ ). S→C males showed higher expression of *Pdc1*, *Aoah*, and *Foxa1* than C→C males following chronic stress exposure (*Pdc1*,  $t_{20} = 2.806$ ,  $P = 0.0109$ ; *Aoah*,  $t_{20} = 3.227$ ,  $P = 0.0042$ ; *Foxa1*,  $t_{20} = 3.277$ ,  $P = 0.0038$ ), and no differences in the expression of these genes between S→C and S→S males. Post hoc analysis also showed that C→S males had higher expression of *Pdc1* than C→C males following chronic stress exposure ( $t_{20} = 2.359$ ,  $P = 0.0286$ ). Data represented as mean  $\pm$  s.e.m. with individual data points overlaid;  $n = 5$  C→C males;  $n = 7$  C→S males;  $n = 7$  S→C males;  $n = 5$  S→S males in all panels.

Following colonization, the bacterial communities within the offspring gut undergo dynamic restructuring that involves complex gene–environment interactions<sup>32</sup>. Despite this, the impact of prenatal stress exposure on bacterial communities within the offspring gut endures across development<sup>10</sup>. We tested the hypothesis that these lasting changes to host–microbe interactions increase the sensitivity of male offspring to the effects of stress on the gut later in life. Consistent with our predictions, stress exposure in adulthood

increased intestinal permeability in S→S males beyond the effect of chronic stress on intestinal permeability that was observed in all treatment groups. As the gut microbiome plays a role in intestinal permeability regulation<sup>2,9</sup>, we adapted rank–rank hypergeometric overlap analysis to assess how stress exposure across treatment groups resulted in similar remodeling of gut microbiota community composition. This approach revealed a common cluster of microbiota altered by stress across treatment groups, as well as distinct microbiota patterns

unique to each treatment group, including enrichment of bacterial species involved in inflammation (*S. lentus*) and depletion of species involved in the maintenance of barrier functions (*L. reuteri*) in S→S males compared to C→C males. These results suggest that maternal stress programming of offspring host–microbe interactions may contribute to long-lasting effects that are at least partially mediated by initial changes in the maternal vaginal microbiota.

We also assessed whether maternal vaginal microbiota contribute to prenatal-stress-induced changes in the PVN, the hypothalamic regulator of the hypothalamic–pituitary–adrenal stress axis<sup>43,44</sup>, in male mice that had undergone adulthood stress. GSEA revealed a robust enrichment of energy metabolism and neurotrophin signaling pathway gene sets in C→C males exposed to adulthood stress relative to S→S males exposed to adulthood stress. These findings may reflect deficits in neuroplasticity following stress in S→S males, which would affect the ability to respond and adapt to stimuli, although the observed differences may also be present in C→C males not exposed to adulthood stress (this condition was not included in this experiment). Consistently, we showed that downregulation of neurotrophin signaling pathways was associated with upregulation of transcripts involved in the regulation of the immune response (i.e., *Mefv*, *Pdcd1*, *Aoah*, *Foxa1*), consistent with previous reports demonstrating a balance between neurotrophic factors and the immune system in the control of inflammation here<sup>44</sup>. Further, we examined whether the intermediate stress sensitivity in S→C males (Fig. 2d) was associated with altered PVN gene expression and found that some genes that were differentially expressed in S→S males versus C→C males were also differentially expressed in S→C males versus C→C males. This suggests that transmission of the prenatal-stress-altered maternal microbiome had lasting effects on PVN gene expression assessed after exposure to chronic stress.

Together, our findings demonstrate that the maternal vaginal microbiome mediates offspring corticosterone responses to stress, body weight development, and hypothalamic gene expression. Further, prenatal stress altered the fetal intestinal niche, which in turn may determine which microbiota can successfully establish residence in the offspring gut during the postnatal window. If the altered fetal intestinal niche prevents successful establishment of transplanted vaginal microbiota, this may explain why inoculation with vaginal microbiome from control dams could not fully rescue the phenotype of prenatally stressed mice (C→S). Together, these findings further increase our understanding of the mechanisms by which maternal stress during pregnancy influences the offspring gut and hypothalamus and thereby possibly increase risk of neurodevelopmental and gastrointestinal disorders.

## Methods

Methods, including statements of data availability and any associated accession codes and references, are available at <https://doi.org/10.1038/s41593-018-0182-5>.

Received: 5 December 2017; Accepted: 23 May 2018;  
Published online: 9 July 2018

## References

- Bale, T. L. et al. Early life programming and neurodevelopmental disorders. *Biol. Psychiatry* **68**, 314–319 (2010).
- Cryan, J. F. & Dinan, T. G. Mind-altering microorganisms: the impact of the gut microbiota on brain and behaviour. *Nat. Rev. Neurosci.* **13**, 701–712 (2012).
- Sampson, T. R. & Mazmanian, S. K. Control of brain development, function, and behavior by the microbiome. *Cell Host Microbe* **17**, 565–576 (2015).
- Gur, T. L. et al. Prenatal stress affects placental cytokines and neurotrophins, commensal microbes, and anxiety-like behavior in adult female offspring. *Brain Behav. Immun.* **64**, 50–58 (2017).
- Golubeva, A. V. et al. Prenatal stress-induced alterations in major physiological systems correlate with gut microbiota composition in adulthood. *Psychoneuroendocrinology* **60**, 58–74 (2015).
- Zijlmans, M. A., Korpela, K., Riksen-Walraven, J. M., de Vos, W. M. & Weerth, C. Maternal prenatal stress is associated with the infant intestinal microbiota. *Psychoneuroendocrinology* **53**, 233–245 (2015).
- Jašarević, E., Morrison, K. E. & Bale, T. L. Sex differences in the gut microbiome–brain axis across the lifespan. *Phil. Trans. R. Soc. Lond. B* **371**, 20150122 (2016).
- Yatsunenkov, T. et al. Human gut microbiome viewed across age and geography. *Nature* **486**, 222–227 (2012).
- Borre, Y. E. et al. Microbiota and neurodevelopmental windows: implications for brain disorders. *Trends Mol. Med.* **20**, 509–518 (2014).
- Jašarević, E., Howard, C. D., Misisic, A. M., Beiting, D. P. & Bale, T. L. Stress during pregnancy alters temporal and spatial dynamics of the maternal and offspring microbiome in a sex-specific manner. *Sci. Rep.* **7**, 44182 (2017).
- Jašarević, E., Howerton, C. L., Howard, C. D. & Bale, T. L. Alterations in the vaginal microbiome by maternal stress are associated with metabolic reprogramming of the offspring gut and brain. *Endocrinology* **156**, 3265–3276 (2015).
- Bronson, S. L. & Bale, T. L. Prenatal stress-induced increases in placental inflammation and offspring hyperactivity are male-specific and ameliorated by maternal antiinflammatory treatment. *Endocrinology* **155**, 2635–2646 (2014).
- Mueller, B. R. & Bale, T. L. Impact of prenatal stress on long term body weight is dependent on timing and maternal sensitivity. *Physiol. Behav.* **88**, 605–614 (2006).
- Mueller, B. R. & Bale, T. L. Early prenatal stress impact on coping strategies and learning performance is sex dependent. *Physiol. Behav.* **91**, 55–65 (2007).
- Mueller, B. R. & Bale, T. L. Sex-specific programming of offspring emotionality after stress early in pregnancy. *J. Neurosci.* **28**, 9055–9065 (2008).
- Pankevich, D. E., Mueller, B. R., Brockel, B. & Bale, T. L. Prenatal stress programming of offspring feeding behavior and energy balance begins early in pregnancy. *Physiol. Behav.* **98**, 94–102 (2009).
- Dominguez-Bello, M. G. et al. Delivery mode shapes the acquisition and structure of the initial microbiota across multiple body habitats in newborns. *Proc. Natl Acad. Sci. USA* **107**, 11971–11975 (2010).
- Dominguez-Bello, M. G. et al. Partial restoration of the microbiota of cesarean-born infants via vaginal microbial transfer. *Nat. Med.* **22**, 250–253 (2016).
- Ericsson, A. C. & Franklin, C. L. Manipulating the gut microbiota: methods and challenges. *ILAR J.* **56**, 205–217 (2015).
- Bravo, J. A. et al. Ingestion of Lactobacillus strain regulates emotional behavior and central GABA receptor expression in a mouse via the vagus nerve. *Proc. Natl Acad. Sci. USA* **108**, 16050–16055 (2011).
- Buffington, S. A. et al. Microbial reconstitution reverses maternal diet-induced social and synaptic deficits in offspring. *Cell* **165**, 1762–1775 (2016).
- Ait-Belgnaoui, A. et al. Prevention of gut leakiness by a probiotic treatment leads to attenuated HPA response to an acute psychological stress in rats. *Psychoneuroendocrinology* **37**, 1885–1895 (2012).
- Ait-Belgnaoui, A. et al. Probiotic gut effect prevents the chronic psychological stress-induced brain activity abnormality in mice. *Neurogastroenterol. Motil.* **26**, 510–520 (2014).
- Wells, J. M. Immunomodulatory mechanisms of lactobacilli. *Microb. Cell Fact.* **10**(Suppl 1), S17 (2011).
- Makarova, K. et al. Comparative genomics of the lactic acid bacteria. *Proc. Natl Acad. Sci. USA* **103**, 15611–15616 (2006).
- Almirón, M., Traglia, G., Rubio, A. & Sanjuan, N. Colonization of the mouse upper gastrointestinal tract by lactobacillus murinus: a histological, immunocytochemical, and ultrastructural study. *Curr. Microbiol.* **67**, 395–398 (2013).
- Howerton, C. L., & Bale, T. L. Targeted placental deletion of OGT recapitulates the prenatal stress phenotype including hypothalamic mitochondrial dysfunction. *Proc. Natl Acad. Sci. USA* **111**, 9639–9644 (2014).
- Rawls, J. F., Mahowald, M. A., Ley, R. E. & Gordon, J. I. Reciprocal gut microbiota transplants from zebrafish and mice to germ-free recipients reveal host habitat selection. *Cell* **127**, 423–433 (2006).
- Akira, S. & Takeda, K. Toll-like receptor signalling. *Nat. Rev. Immunol.* **4**, 499–511 (2004).
- Deshmukh, H. S. et al. The microbiota regulates neutrophil homeostasis and host resistance to *Escherichia coli* K1 sepsis in neonatal mice. *Nat. Med.* **20**, 524–530 (2014).
- Molloy, M. J. et al. Intraluminal containment of commensal outgrowth in the gut during infection-induced dysbiosis. *Cell Host Microbe* **14**, 318–328 (2013).
- Rakoff-Nahoum, S. et al. Analysis of gene–environment interactions in postnatal development of the mammalian intestine. *Proc. Natl Acad. Sci. USA* **112**, 1929–1936 (2015).
- Cani, P. D. et al. Changes in gut microbiota control metabolic endotoxemia-induced inflammation in high-fat diet-induced obesity and diabetes in mice. *Diabetes* **57**, 1470–1481 (2008).

34. Seo, S. U. et al. Distinct commensals induce interleukin-1 $\beta$  via NLRP3 inflammasome in inflammatory monocytes to promote intestinal inflammation in response to injury. *Immunity* **42**, 744–755 (2015).
35. Nemegehaire, S. et al. The ecological importance of the *Staphylococcus sciuri* species group as a reservoir for resistance and virulence genes. *Vet. Microbiol.* **171**, 342–356 (2014).
36. Ahrne, S. & Hagslatt, M. L. Effect of lactobacilli on paracellular permeability in the gut. *Nutrients* **3**, 104–117 (2011).
37. Houghteling, P. D. & Walker, W. A. Why is initial bacterial colonization of the intestine important to infants' and children's health? *J. Pediatr. Gastroenterol. Nutr.* **60**, 294–307 (2015).
38. Bailey, M. T. & Coe, C. L. Maternal separation disrupts the integrity of the intestinal microflora in infant rhesus monkeys. *Dev. Psychobiol.* **35**, 146–155 (1999).
39. Bailey, M. T., Lubach, G. R. & Coe, C. L. Prenatal stress alters bacterial colonization of the gut in infant monkeys. *J. Pediatr. Gastroenterol. Nutr.* **38**, 414–421 (2004).
40. Winter, S. E. & Bäumlner, A. J. Why related bacterial species bloom simultaneously in the gut: principles underlying the 'Like will to like' concept. *Cell. Microbiol.* **16**, 179–184 (2014).
41. Gomez de Agüero, M. et al. The maternal microbiota drives early postnatal innate immune development. *Science* **351**, 1296–1302 (2016).
42. Mayer, E. A. The neurobiology of stress and gastrointestinal disease. *Gut* **47**, 861–869 (2000).
43. Mayer, E. A. Gut feelings: the emerging biology of gut-brain communication. *Nat. Rev. Neurosci.* **12**, 453–466 (2011).
44. Kerschensteiner, M., Stadelmann, C., Dechant, G., Wekerle, H. & Hohlfeld, R. Neurotrophic cross-talk between the nervous and immune systems: implications for neurological diseases. *Ann. Neurol.* **53**, 292–304 (2003).

### Acknowledgements

The research reported in this publication was supported by a pilot award from the PennVet Center for Host–Microbial Interactions at the University of Pennsylvania.

T.L.B. was supported by the National Institutes of Mental Health under Award Numbers P50-MH099910, MH 104184, MH 091258, MH 087597, MH 073030, and MH 108286. E.J. was supported by the National Institutes of Health National Research Service Award F32 MH 109298. T.W. was supported by National Institutes of Health Postdoctoral Research Grant F32 AI 114080.

### Author contributions

E.J. and T.L.B. designed the experiments and wrote the manuscript. E.J. performed the cesarean delivery experiments, molecular biology experiments, and behavioral experiments and performed bioinformatics analysis of RNA-seq data, 16S rRNA marker gene sequencing data, and whole-metagenomic shotgun sequencing data. C.D.H. assisted with all cesarean delivery experiments. A.M.M. and D.P.B. provided bioinformatics support for RNA-seq, 16S rRNA, and shotgun whole-metagenomics. K.E.M. collected PVN brain micropunches for RNA-seq analyses. T.W. conducted fetal intestine cell isolation and flow cytometry analyses. T.W., P.S., and C.A.H. provided resources and equipment for multicolor flow cytometry of fetal intestinal tissues. All authors contributed to manuscript editing and revision.

### Competing interests

The authors declare no competing interests.

### Additional information

**Supplementary information** is available for this paper at <https://doi.org/10.1038/s41593-018-0182-5>.

**Reprints and permissions information** is available at [www.nature.com/reprints](http://www.nature.com/reprints).

**Correspondence and requests for materials** should be addressed to T.L.B.

**Publisher's note:** Springer Nature remains neutral with regard to jurisdictional claims in published maps and institutional affiliations.

## Methods

**Experimental animals.** Mice used in these studies were on a mixed C57BL/6:129 background and were maintained in-house as an outbred mixed colony. A total of 200 mixed-colony breeding pairs were used for these studies, and females were checked daily at 700 EST for copulation plugs. Dams were housed under a 12-h light/day photoperiod with a standard chow diet (Purina Rodent Chow, St. Louis, MO; 28.1% protein, 59.8% carbohydrate, 12.1% fat) and ad libitum access to water. Noon on the day that the plug was observed was considered to be E0.5. Samples from one male and one female per litter were used for all subsequent analyses. All experiments were approved by the University of Pennsylvania Institutional Animal Care and Use Committee and performed in accordance with National Institutes of Health Animal Care and Use Guidelines.

**Early prenatal stress.** Administration of chronic variable stress was performed as previously described<sup>12–16,27</sup>. Dams were randomly assigned to treatment groups to receive stress during days 1–7 of gestation (prenatal stress;  $n=70$ ) or to a control ( $n=70$ ) unstressed group. An additional 60 foster females were time-mated and used for cesarean delivery and cross-foster experiments. Following confirmation of a copulation plug, pregnant mice assigned to the prenatal stress group experienced each of the following stressors on different days: 60 min of fox odor exposure (1:5,000 2,4,5-trimethylthiazole; Acros Organics), 15 min of restraint (beginning at 1300 EST) in a modified 50-mL conical tube, 36 h of constant light, novel noise (White Noise/Nature Sound-Sleep Machine; Brookstone) overnight, three cage changes throughout the light cycle, saturated bedding (700 mL, 23°C water) overnight, and novel object exposure (eight marbles of similar shape and color) overnight. Stressors were selected to be nonhabituating and did not induce pain or directly influence maternal food intake, weight gain, behavior, litter size, or sex ratio<sup>12–16,27</sup>.

**Cesarean surgeries.** Donor and foster females were time-mated, and 24 h before expected delivery (E18.5), vaginal fluid was collected from donor dams with 200  $\mu$ L of sterile saline and the entire contents of the pipette were expelled into the tube, which remained at room temperature (22 °C) until neonatal gavage. Immediately following vaginal lavaging, cesarean deliveries of offspring were conducted under sterile conditions according to established protocols for generating germ-free offspring, with modifications<sup>45,46</sup>. Cesarean delivery was modified in the following manner: immediately following rapid decapitation, dams were submerged in 100% EtOH for 30 s and the dam's abdomen was wiped down with Betadine to minimize contamination of the uterine horn from maternal skin bacteria during extraction. Following removal, uterine horns were placed on a sterile field inside a sterile incubator. Once the fetus and placenta were expelled from the uterine horn, the placenta and membranes that surround the pups were removed and the umbilical cord was ligated. The remaining membranes and fluid from the nose and mouth of the pup were cleared, and after breathing was stimulated, pups were kept warm on a sterile field inside a separate sterile incubator. Time from decapitation to stimulation of breathing was 5 min. Orogastric gavage occurred by guiding a silastic catheter (Intramedic Polyethylene Tubing PE 10, Becton Dickinson, Franklin Lakes, NJ) into the neonate's esophagus, upon which offspring were fed once with 15  $\mu$ L of maternal vaginal fluid. Noninoculated offspring remained in the sterile incubator until fostering. To control for the contribution of the postnatal environment in offspring bacterial colonization, offspring from all treatment groups were fostered to the same foster dam. All animals exhibited a milk dot at time of P2 collection, indicating successful feeding and acceptance of pup by the foster mother. Distal colon samples were collected 48 h following inoculation, when the animals were considered P2. Distal colons were collected from a separate age-matched cohort of vaginally delivered offspring at P2. It is important to note that we controlled for prenatal litter effects by transferring only 1 male and 1 female offspring from a given cesarean section donor female to a foster female. In addition, offspring with overt signs of developmental delay, including small size relative to litters or presence of a neighboring resorption site, were excluded.

**Light–dark box.** The light–dark box test was performed as described previously<sup>47,48</sup>. Adult mice were placed in the light compartment at the beginning of the 10-min test session. Light intensities were set at 5 lx in the dark compartment and 300 lx in the light compartment. All testing occurred 2–5 h after lights off. Total time spent in the light compartment and the number of light-to-dark transitions were analyzed with ANY-maze v4.75 software (Stoelting). The observer was blind to the experimental treatment of each animal.

**Hypothalamic–pituitary–adrenal stress axis assessment.** Cesarean-delivered and cross-fostered vaginally delivered 10- to 11-week-old male and female mice were restrained in animal restrainers for 15 min beginning at time 0 and were immediately returned to their home cage at the conclusion of restraint. As previously described, a single tail snip was made at time 0, removing < 1 mm tissue from the distal tip. A total of 10  $\mu$ L tail blood was collected by micropipette at 0, 15, 30, and 120 min into EDTA-treated tubes, first blotting the blood clot and then gently milking the tail to stimulate blood flow<sup>49</sup>. Corticosterone levels were

determined by radioimmunoassay (MP Biomedicals) in 3  $\mu$ L plasma. All testing was completed 2–5 h after lights on. The observer was blind to the experimental treatment of each animal.

**Chronic variable stress.** Administration of chronic variable stress in adult males was performed as described previously<sup>13</sup>. Briefly, seven different stressors were randomized and administered one per day. Stressors were selected based on previous observations that they are nonhabituating, do not induce pain, and do not affect food or water intake, and included the following: 36 h constant light, 15-min exposure to fox odor (1:5,000, 2,4,5-trimethylthiazole; Acros Organics), novel object (marbles) overnight, 15-min restraint in a 50-mL conical tube, multiple cage changes, novel 100 dB white noise (Sleep Machine; Brookstone) overnight, and saturated bedding overnight.

**Intestinal permeability assay.** Immediately following the last day of chronic stress exposure, mice were fasted for 4 h before receiving an oral gavage with 0.6 g/kg 4-kDa FITC-dextran (Sigma Aldrich). Four hours later, serum samples were read for fluorescence intensity at 521 nm using an xFluor4 spectrometer (Tecan).

**16S rRNA marker-gene sequencing and analysis.** Genomic DNA from fecal, vaginal, and colon samples were isolated using the Stratec PSP Spin Stool DNA Plus kit using the manufacturer's protocol for difficult-to-lyse bacteria (STRATEC Molecular GmbH, Berlin, Germany). The V4 region of the 16S rRNA gene was amplified using barcoded primers for the Illumina platform, as previously described<sup>50</sup>. Sequencing was performed on a MiSeq instrument (Illumina, San Diego, CA) using 250-base paired-end chemistry at the University of Pennsylvania Next Generation Sequencing Core. Paired-end reads were assembled and quality-filtered to include sequences with  $Q \geq 30$ . Mothur v. 1.36.1 was employed to remove sequences <248 bp and >255 bp in length and sequences with homopolymers >10 bp in length<sup>51</sup>. QIIME v. 1.8 was used for further downstream processing and analyses<sup>52</sup>. OTUs were defined using 97% sequence similarity with CD-HIT, and a representative sequence from each OTU containing  $\geq 10$  sequences was chosen for downstream analyses (based on the most abundant sequence). Chimeric sequences were removed using ChimeraSlayer. Representative sequences were assigned to genera using the Ribosomal Database Project (RDP) classifier v 2.2, multiple sequence alignment was performed using PyNAST, and phylogeny was built with FastTree. The samples were rarified to 1,000 sequences per sample for calculating alpha- and beta-diversity metrics.

**Whole–metagenomic shotgun sequencing and analysis.** Genomic DNA from fecal and colon samples were isolated using the Stratec PSP Spin Stool DNA Plus kit using the manufacturer's protocol for difficult-to-lyse bacteria (STRATEC Molecular GmbH, Berlin, Germany). Illumina paired-end DNA libraries of colonic and fecal samples were prepared from 0.2 ng gDNA using the Nextera XT DNA library prep kit (FC-131-1096, Illumina) according to the manufacturer's protocol. Biological replicates were multiplexed and sequenced on four identical NextSeq500 lanes using high-output 2 $\times$  150-bp chemistry (Illumina). Sequence generated FASTQ files were concatenated, and subsequent alignments and classifications were confirmed using the software tool from OneCodex, which contains a dataset that includes 30,825 bacterial reference genomes compared with the 2,948 bacterial reference genomes NCBI RefSeq Complete Genomes database. To account for high sparsity common in metagenomics datasets, we applied cumulative-sum scaling normalization implemented in the metagenomeSeq Bioconductor package to our datasets<sup>53</sup>. Normalized log<sub>2</sub> counts were tested for differential abundance using limma v.3.12.3<sup>54</sup>.

**RNA-seq of E18.5 fetal intestinal tracts.** On E18.5, pregnant dams were rapidly decapitated by cervical dislocation. Litter characteristics, such as intrauterine position, number of offspring, sex ratio, and resorption sites, were noted. Tail snip from embryos were collected and retained for determination of sex by genotyping using primers specific to *Jarid1* (5'-TGAAGCTTTTGGCTTTGAG-3' and 5'-CCGCTGCCAAATCTTTTG-3'), as described elsewhere<sup>12</sup>. Fetal intestinal tracts were rapidly frozen in liquid nitrogen and maintained in –80 °C until RNA isolation. To control for the significant contribution of uterine horn laterality and intrauterine position, we selected fetal intestinal tract samples from conceptuses that were required to be from the first third of the embryos from cervical end; female samples flanked by two males (2M females) were excluded, and embryos could not exhibit overt signs of developmental delay (for example, small size relative to litters and no presence of a neighboring resorption site). Messenger RNA was purified using an RNeasy Mini kit (Qiagen). Illumina single-end cDNA libraries of E18.5 fetal intestinal tract mRNA were prepared from 250 ng total RNA using the TruSeq Stranded mRNA Kit with poly-A enrichment (RS-122-2101, Illumina) according to the manufacturer's protocol. Library fragment size was quantified using an Agilent High Sensitivity D100 ScreenTape Assay on an Agilent 4200 TapeStation System (G2991AA). Library concentration was quantified using the Qubit dsDNA HS (High Sensitivity) Assay Kit. Samples representative of all treatment groups were multiplexed and sequenced on NextSeq500 lanes using high-output 1 $\times$  75-bp geometry (Illumina).

**Flow cytometry.** On E18.5, pregnant dams were rapidly decapitated by cervical dislocation. To account for sex-specific effects of prenatal stress on immune cell populations, tail snips from embryos were collected and retained for determination of sex by genotyping using primers specific to *Jarid1* (5'-TGAAGCTTTGGCTTTGAG-3' and 5'-CCGCTGCCAAATCTTTGG-3'), as described elsewhere<sup>12</sup>. E18.5 fetal intestines and adult spleens were mechanically disrupted in Hanks' Balanced Salt Solution (Sigma-Aldrich, St. Louis, MO) enriched with 5% FBS and 30 mM HEPES. Cells were incubated with fixable Aqua dye (Invitrogen, Carlsbad, CA) to assess viability. For cell-surface molecules, FcRs were blocked with CD16/32 (Cat. # 14-0161-8, eBioscience, San Diego, CA), and cells were stained using  $\alpha$ -CD45-AF700 (Clone 30-F11, Cat. #56-0451-82, eBioscience),  $\alpha$ -Ly6C-PerCPy5.5 (Clone HK1.4, Cat. #45-5932-80, eBioscience),  $\alpha$ -Ly6G-APC (Clone 1A8, Cat. #117-9668-80, eBioscience), and  $\alpha$ -CD11b-BV605 (M1/70, Cat. #101237, BioLegend, San Diego, CA). For intracellular cytokine staining, splenic cells were fixed with 2% paraformaldehyde (Electron Microscopy Sciences), permeabilized with 0.2% saponin buffer, and stained with anti-TNF- $\alpha$  (Cat. #901201, BioLegend). Cell events were acquired on LSRII Fortessa flow cytometers (BD Biosciences, San Jose, CA) and analyzed using FlowJo (Tree Star, Ashland, OR).

**RNA-seq analysis of the adult PVN.** Messenger RNA was purified RNeasy Mini kit (Qiagen). Illumina single-end cDNA libraries of adult male PVN mRNA were prepared from 250 ng total RNA using the TruSeq Stranded mRNA Kit with poly-A enrichment (RS-122-2101, Illumina) according to the manufacturer's protocol. Five to seven biological replicates per group (24 total cDNA libraries) were multiplexed and sequenced on two identical NextSeq500 lanes using high-output 1×75-bp chemistry (Illumina). The concatenated FASTQ files generated from Illumina were used as input to kallisto, a program that pseudoaligns high-throughput sequencing reads to the *Mus musculus* reference transcriptome (version 38) and quantifies transcript expression<sup>35</sup>. We used 60 bootstrap samples to ensure accurate transcript quantification. Gene isoforms were collapsed to gene symbols using the Bioconductor package tximport (version 3.4)<sup>36</sup>. Counts were normalized using voom, and normalized counts were tested for differential abundance using limma v.3.12.3<sup>34,37</sup>.

**Fetal intestinal messenger RNA analysis.** Messenger RNA was purified RNeasy Mini kit (Qiagen) from male and female fetal intestine samples at E18.5. cDNA was transcribed using the HighCapacity cDNA reverse transcriptase kit (Applied Biosystems). Changes in intestinal tumor necrosis factor- $\alpha$  (Tnfa, NM\_001278601.1, Mm00443258\_m1) were measured by quantitative real-time PCR using TaqMan gene expression assays (Applied Biosystems). Samples were run in triplicate for the target genes and endogenous controls (Actb, NM\_007393.3, Mm00607939\_s1) on the same 96-well plate. Analysis was performed by the comparative Ct method, and expression levels were normalized to control male offspring<sup>38</sup>.

**Statistical analyses.** Data are reported as mean  $\pm$  s.e.m. in bar plots and as box-and-whisker plots. All mice were from a mixed C57BL/6:129 background, and sex and age are noted in the individual figure legends. No statistical methods were used to predetermine sample sizes, but our sample sizes are similar to those reported in previous publications using the early-prenatal-stress mouse model<sup>10–16</sup>. No samples or data points were excluded. Assumptions regarding normality were made based on the dataset associated with each experiment. Data generated from 16S rRNA marker gene sequencing are nonparametric, and nonparametric statistical analyses were used. For the other datasets, distribution was assumed to be normal, but this was not formally tested. The investigators were blinded to the treatment of the mice in individual experiments, with the exception of the cesarean surgery experiments where administration of treatment-specific maternal vaginal microbiota samples was essential for the experiments. Experiment order was not randomized. Animals assigned to treatment groups during cesarean delivery were randomized. Animals assigned to control or chronic stress treatment groups in the second-hit experiments were randomized. Prenatal litter effects were controlled by transferring only 1 male and 1 female offspring from a given cesarean section donor female to a foster female. Growth curves and corticosterone levels were analyzed by two-way ANOVA with time as a repeated measure. P70, corticosterone

AUC, light–dark box behavioral data were analyzed within-sex by one-way ANOVA. Two-sided Tukey's and two-sided Fisher's LSD tests were used for post hoc pairwise comparisons. Permutational multivariate analysis of variance using distance matrices (PERMANOVA) was used to analyze effects of cesarean delivery and inoculation on unweighted UniFrac distances and PERMANOVA *P* values are based on 999 Monte Carlo simulations. Statistical significance was set at  $\alpha=0.05$ . Rank–rank hypergeometric overlap analysis assessed the overlap of microbiota composition between treatment groups following chronic variable stress exposure, as previously described<sup>39</sup>. GSEA (v2.0, Broad Institute) was conducted with the standardized threshold of FDR < 0.25. Statistical analyses for corticosterone levels, body weight, and behavioral tests were performed in GraphPad Prism for Mac OS X (version 6.00, GraphPad Software). All other statistical analyses were conducted within the R environment using Bioconductor packages<sup>40</sup>.

**Reporting Summary.** Further information on experimental design is available in the Nature Research Reporting Summary linked to this article.

**Data availability.** The data that support the findings of this study are available from the corresponding author upon reasonable request.

## References

- Nagy, A., Gertsenstein, M., Vintersten, K. & Behringer, R. Cesarean section and fostering. *CSH Protocols* **2006**, pdb.prot4381 (2006).
- Murphy, D. Cesarean section and fostering. *Methods Mol. Biol.* **18**, 177–178 (1993).
- McEuen, J. G., Semsar, K. A., Lim, M. A. & Bale, T. L. Influence of sex and corticotropin-releasing factor pathways as determinants in serotonin sensitivity. *Endocrinology* **150**, 3709–3716 (2009).
- Bale, T. L. et al. Mice deficient for corticotropin-releasing hormone receptor-2 display anxiety-like behaviour and are hypersensitive to stress. *Nat. Genet.* **24**, 410–414 (2000).
- Rodgers, A. B., Morgan, C. P., Bronson, S. L., Revello, S. & Bale, T. L. Paternal stress exposure alters sperm microRNA content and reprograms offspring HPA stress axis regulation. *J. Neurosci.* **33**, 9003–9012 (2013).
- Kozich, J. J., Westcott, S. L., Baxter, N. T., Highlander, S. K. & Schloss, P. D. Development of a dual-index sequencing strategy and curation pipeline for analyzing amplicon sequence data on the MiSeq Illumina sequencing platform. *Appl. Environ. Microbiol.* **79**, 5112–5120 (2013).
- Schloss, P. D. et al. Introducing mothur: open-source, platform-independent, community-supported software for describing and comparing microbial communities. *Appl. Environ. Microbiol.* **75**, 7537–7541 (2009).
- Caporaso, J. G. et al. QIIME allows analysis of high-throughput community sequencing data. *Nat. Methods* **7**, 335–336 (2010).
- Paulson, J. N., Stine, O. C., Bravo, H. C. & Pop, M. Differential abundance analysis for microbial marker-gene surveys. *Nat. Methods* **10**, 1200–1202 (2013).
- Ritchie, M. E. et al. limma powers differential expression analyses for RNA-sequencing and microarray studies. *Nucleic Acids Res.* **43**, e47 (2015).
- Bray, N. L., Pimentel, H., Melsted, P. & Pachter, L. Near-optimal probabilistic RNA-seq quantification. *Nat. Biotechnol.* **34**, 525–527 (2016).
- Soneson, C., Love, M. I. & Robinson, M. D. Differential analyses for RNA-seq: transcript-level estimates improve gene-level inferences. *F1000Res.* **4**, 1521 (2015).
- Law, C. W., Chen, Y., Shi, W. & Smyth, G. K. voom: precision weights unlock linear model analysis tools for RNA-seq read counts. *Genome Biol.* **15**, R29 (2014).
- Schmittgen, T. D. & Livak, K. J. Analyzing real-time PCR data by the comparative C(T) method. *Nat. Protoc.* **3**, 1101–1108 (2008).
- Plaisier, S. B., Taschereau, R., Wong, J. A. & Graeber, T. G. Rank–rank hypergeometric overlap: identification of statistically significant overlap between gene-expression signatures. *Nucleic Acids Res.* **38**, e169 (2010).
- RC Team. *R: a Language and Environment for Statistical Computing*. (R Foundation for Statistical Computing, Vienna, Austria, 2014).

## Reporting Summary

Nature Research wishes to improve the reproducibility of the work that we publish. This form provides structure for consistency and transparency in reporting. For further information on Nature Research policies, see [Authors & Referees](#) and the [Editorial Policy Checklist](#).

### Statistical parameters

When statistical analyses are reported, confirm that the following items are present in the relevant location (e.g. figure legend, table legend, main text, or Methods section).

n/a Confirmed

- The exact sample size ( $n$ ) for each experimental group/condition, given as a discrete number and unit of measurement
- An indication of whether measurements were taken from distinct samples or whether the same sample was measured repeatedly
- The statistical test(s) used AND whether they are one- or two-sided  
*Only common tests should be described solely by name; describe more complex techniques in the Methods section.*
- A description of all covariates tested
- A description of any assumptions or corrections, such as tests of normality and adjustment for multiple comparisons
- A full description of the statistics including central tendency (e.g. means) or other basic estimates (e.g. regression coefficient) AND variation (e.g. standard deviation) or associated estimates of uncertainty (e.g. confidence intervals)
- For null hypothesis testing, the test statistic (e.g.  $F$ ,  $t$ ,  $r$ ) with confidence intervals, effect sizes, degrees of freedom and  $P$  value noted  
*Give  $P$  values as exact values whenever suitable.*
- For Bayesian analysis, information on the choice of priors and Markov chain Monte Carlo settings
- For hierarchical and complex designs, identification of the appropriate level for tests and full reporting of outcomes
- Estimates of effect sizes (e.g. Cohen's  $d$ , Pearson's  $r$ ), indicating how they were calculated
- Clearly defined error bars  
*State explicitly what error bars represent (e.g. SD, SE, CI)*

*Our web collection on [statistics for biologists](#) may be useful.*

### Software and code

Policy information about [availability of computer code](#)

Data collection

No software was used.

Data analysis

No custom software and codes were used. Data analyses were performed with the R environment, Bioconductor, and GraphPad Prism 7. Experiments with two groups were analyzed statistically using two-tailed Student's  $t$ -tests. Experiments with more than two groups were subjected to one-way ANOVA, two-way ANOVA, or two-way repeated measure ANOVA (rmANOVA), followed by post hoc tests. We described this in the Method section of the manuscript, and the statistical used for each figure panel is described in the corresponding figure legend. mothur v. 1.36.1 was employed to remove sequences and homopolymers. QIIME v. 1.8 was used for standardized processing and analyses. OTUs were defined using CD-HIT. FastTree was used to build phylogeny. OneCodex is commercially available was used for annotating and quantifying sequence counts. FlowJo is commercially available was used to identify immune cell populations and analyze frequencies.

For manuscripts utilizing custom algorithms or software that are central to the research but not yet described in published literature, software must be made available to editors/reviewers upon request. We strongly encourage code deposition in a community repository (e.g. GitHub). See the Nature Research [guidelines for submitting code & software](#) for further information.

## Data

Policy information about [availability of data](#)

All manuscripts must include a [data availability statement](#). This statement should provide the following information, where applicable:

- Accession codes, unique identifiers, or web links for publicly available datasets
- A list of figures that have associated raw data
- A description of any restrictions on data availability

The data that support the findings of this study are available from the corresponding author upon reasonable request.

## Field-specific reporting

Please select the best fit for your research. If you are not sure, read the appropriate sections before making your selection.

Life sciences       Behavioural & social sciences       Ecological, evolutionary & environmental sciences

For a reference copy of the document with all sections, see [nature.com/authors/policies/ReportingSummary-flat.pdf](https://www.nature.com/authors/policies/ReportingSummary-flat.pdf)

## Life sciences study design

All studies must disclose on these points even when the disclosure is negative.

Sample size	Sample size was based on literature in the field and based the corresponding author's 16 years of experience conducting these experiments and using this particular mouse model.
Data exclusions	No data was excluded in analysis.
Replication	We listed the number of times we repeated the experiments in figure legends. Each biological replicate was conducted in unrelated animals, non-litter mates, and each replicate was conducted at different time points, therefore ensuring the durability of effects. All attempts at replication were successful.
Randomization	For the inoculation experiments, one male and one female pup selected per litter for inoculation was randomized. Pregnant females were randomly assigned to stress or no stress groups. For adult stress experiments, mice of different treatment groups were randomly assigned to no stress/stress groups. The male and female pup collected for RNA-Seq and flow cytometry experiments was randomized.
Blinding	Data collection was conducted with experimenter blind to treatment. Data was coded such that analysis was conducted blind.

## Reporting for specific materials, systems and methods

### Materials & experimental systems

n/a	Involvement in the study
<input checked="" type="checkbox"/>	<input type="checkbox"/> Unique biological materials
<input type="checkbox"/>	<input checked="" type="checkbox"/> Antibodies
<input checked="" type="checkbox"/>	<input type="checkbox"/> Eukaryotic cell lines
<input checked="" type="checkbox"/>	<input type="checkbox"/> Palaeontology
<input type="checkbox"/>	<input checked="" type="checkbox"/> Animals and other organisms
<input checked="" type="checkbox"/>	<input type="checkbox"/> Human research participants

### Methods

n/a	Involvement in the study
<input checked="" type="checkbox"/>	<input type="checkbox"/> ChIP-seq
<input type="checkbox"/>	<input checked="" type="checkbox"/> Flow cytometry
<input checked="" type="checkbox"/>	<input type="checkbox"/> MRI-based neuroimaging

## Antibodies

Antibodies used

For flow cytometry experiments:

CD16/CD32 (14-0161-81, eBioscience, 1:200)  
 a-CD45-AF700 (Clone 30-F11, 56-0451-82, eBioscience, 1:100)  
 a-Ly6C-PerCPCy5.5 (Clone HK1.4, 45-5932-80, eBioscience, 1:100)  
 a-Ly6G-APC (Clone 1A8, 117-9668-80, eBioscience, 1:100)  
 a-CD11b-BV605 (M1/70, 101237, BioLegend, 1:100)  
 anti-TNF-a (901201, BioLegend, 1:100)

## Validation

All antibodies used in this study were commercially available and validated by companies. All validation are provided on the product details page of each commercially available antibody.

## Animals and other organisms

Policy information about [studies involving animals](#); [ARRIVE guidelines](#) recommended for reporting animal research

### Laboratory animals

All mice in this study were on a mixed C57BL/6:129 background, and males and females from this mixed colony were used for experiments. E18.5, PN2, PN14, PN21, PN28, PN35, PN42, PN49, PN56, PN63, and PN70 animals of both sexes were used.

### Wild animals

Wild animals were not used.

### Field-collected samples

Field-collected samples were not used.

## Flow Cytometry

### Plots

Confirm that:

- The axis labels state the marker and fluorochrome used (e.g. CD4-FITC).
- The axis scales are clearly visible. Include numbers along axes only for bottom left plot of group (a 'group' is an analysis of identical markers).
- All plots are contour plots with outliers or pseudocolor plots.
- A numerical value for number of cells or percentage (with statistics) is provided.

### Methodology

#### Sample preparation

Embryonic day 18.5 fetal intestines were harvested and mechanically disassociated with a 70  $\mu$ m cell strainer, washed, and samples were labeled with fluorescence conjugated antibody, and analyzed with flow cytometer.

#### Instrument

LSRII Fortessa was used for data collection.

#### Software

FlowJo Version 10 was used for data analysis, and Graphpad Prism 7 for statistical testing.

#### Cell population abundance

The singlet cells were gated according to the FCS/SSC level, CD45+ cells were gated, then CD11b+ cells were gated. CD11b+Ly6G+ cells were defined as relevant cell populations. CD11b+Ly6G-Ly6C+ were defined as relevant cell populations. Described numbers in Figures represent a percentage of CD11b+Ly6G-Ly6C+ and CD11b+Ly6G+ cells in CD11b+ parent cells.

#### Gating strategy

Cells were gated based on the level of SSC-A and FSC-A to exclude cell debris or dead cells. Then, CD45+ cells were further gated, and analyzed. Ly6C+ cells were gated on Ly6G- cells to ensure that the monocyte population of interest did not contain neutrophils.

Tick this box to confirm that a figure exemplifying the gating strategy is provided in the Supplementary Information.